ANALYSIS OF CABLE STAYED BRIDGES FOR FLUTTER WITH GYROSCOPIC ACTIVE CONTROL DEVICE AS TORSIONAL DAMPER

A Dissertation Submitted

In Partial Fulfilment of the Requirements

For the degree of

MASTER OF ENGINEERING

IN

STRUCTURAL ENGINEERING

Submitted by:

BARATH RAGESH P M

(ROLL NO: 801322006)

UNDER THE SUPERVISION OF

DR. NAVEEN KWATRA

Professor and Head

Department of Civil Engineering

Thapar University, Patiala

DEPARTMENT OF CIVIL ENGINEERING

THAPAR UNIVERSITY,

PATIALA-147004

JULY 2015

ANALYSIS OF CABLE STAYED BRIDGES FOR FLUTTER WITH GYROSCOPIC ACTIVE CONTROL DEVICE AS TORSIONAL DAMPER

A Dissertation Submitted

In Partial Fulfilment of the Requirements

For the degree of

MASTERS OF ENGINEERING

IN

STRUCTURAL ENGINEERING

Submitted by:

BARATH RAGESH P M

(ROLL NO: 801322006)

UNDER THE SUPERVISION OF

DR. NAVEEN KWATRA

Professor and Head

Department of Civil Engineering

Thapar University, Patiala

DEPARTMENT OF CIVIL ENGINEERING

THAPAR UNIVERSITY,

PATIALA-147004

JULY 2015

DECLARATION

I, BarathRagesh M, hereby declare that this thesis entitled **"Analysis of Cable Stayed Bridges for Flutter With Gyroscopic Active Control Device as Torsional Damper"** is an authentic record of my study carried out as requirements for the award of degree of **Master of Engineering** in **Structural Engineering** in the Civil Engineering Department, Thapar University, Patiala under the supervision of **Dr. Naveen Kwatra, Professor and Head,** Department of Civil Engineering, Thapar University, Patiala during July 2014 to July 2015. This matter embodied in this report has not been submitted in part or full to any other university or institute for the award of any degree.

Date: July/2015

(BarathRagesh P M)

Roll No. : 801322006

CERTIFICATE

This is to certify that above statement made by the student concerned is correct and true to the best of my knowledge and belief.

17/7/15

Dr. Naveen Kwatra
Professor and Head
Department of Civil Engineering
Thapar University, Patiala

Countersigned by

Dr. S.S Bhatia
Dean of Academic Affairs
Thapar University, Patiala - 147004

ACKNOWLEDGEMENT

A thesis cannot be completed without the help of many people who contributed directly or indirectly through their constructive criticism in the evolution and preparation of this work. It would not be fair on my part, if I don't say a word to thanks to all those whose sincere advice made this period a real educative, enlightening, pleasurable and memorable one.

First of all a special debt of gratitude is owned to my supervisor, **Dr. Naveen kwatra, P**rofessor **and Head** Department of Civil Engineering Thapar University, Patiala for his gracious efforts and keen pursuits, which has remained as a valuable asset for the successful completion of the work. His support and enthusiasm has been highly instrumental in keeping my spirit high.

I would like to express my sincere gratitude to all the staffs of Department of Civil Engineering who guided me throughout the course of study here. And I would also like to thank all my friends whose encouragement and support helped me complete my thesis work in time.

BarathRagesh P M

(801322006)

ABSTRACT

Cable supported bridges are distinguished by their ability to overcome larges spans. At present cable supported bridges are enabled for spans in range from 200m to 2000m, thus covering approximately 90% of the present span range. Even though they have the huge advantage of covering the cost of construction of pylons in deep waters they are not without disadvantages. They high degree of indeterminacy which makes them tough for analysis and also the large spans makes them high susceptible to dynamic loading problems as they have high degree of freedom. Cable supported bridges have reached up to a span of 1991m in Akashi Kaikyo Bridge which is a cable suspended bridge and 1104m in Russky's bridge which is a cable stayed bridge. These bridges have huge span to depth ratio which is the advantage of these bridges in architectural and economic point of view makes them susceptible to aerodynamic forces due to wind loads.

The failure of Tacoma Narrows bridge in November 1940 at very low wind speed of only 64km/hr lead to the new field of wind engineering to be taken seriously. Various researches were done on various aerodynamic forces that would act on structures like along wind response, across wind response of structures, buffeting, vortex shedding, galloping, torsional divergence flutter etc. These researches led to ground breaking achievements in tall structures and long span bridges. With the improvement of heights of building and increasing problems occurred in dynamics of the building. To control the problems occurring in structures various control mechanisms were also introduced with respect to time.

The Gyroscope is equipment that works with principle of "Law of conservation of angular momentum". These are used for various purposes such as leveling instruments, balancing instruments, toys, aerospace industry, shipping etc. In shipping it used in anti roll gyroscopes which helps to reduce the discomfort caused by roll of ship which was caused by wave effect in ships. These equipments were used as early as 1850's in passenger ships to give comfort to passengers. The idea of this project is to use this as the same principle as antiroll gyroscopes to provide torsional damping to the cable stayed bridges to protect the bridges from coupled or classic flutter and single degree of freedom flutter or torsional flutter in low wind velocities.

By providing these dampers and increasing the flutter velocity we can increase the flutter velocity to 71.936 % to that of undamped flutter velocity while increasing the damping by 806.79% The increase in damping ratio might look huge but the damping ratio to the critical varies from 0.2% to 1.8% which is very less compared to normal R.C and steel structures which has damping ratios up to 5% without providing any additional damping device.

CONTENTS

CHAPTER -5

CONCLUSIONS AND RECOMMENDATIONS FOR FUTHER STUDY

LIST OF TABLES

LIST OF FIGURES

1.1 CABLE STAYED BRIDGES

Cable supported bridges are distinguished by their ability to overcome larges spans. At present cable supported bridges are enabled for spans in range from 200m to 2000m, thus covering approximately 90% of the present span range.

There are two types of cable supported systems:

i. Suspended cables systems
ii. Cable stayed systems

The suspension cable system consists of parabolic main cable and vertical hanger cables connecting the deck to the main cable. The most common suspension bridge system has three spans. A larger main span flanked by shorter side spans. The three span bridges is in most cases symmetrical with side spans of equal size. There are other cases also which has only main span and no side span.

The cable stayed system contains straight cables connecting the deck to the pylons. It can be either connected by means of fan system where all the cables radiate from the pylon top or harp system where cable stays are parallel. Besides these two systems a semi harp semi fan system can also be used where cables radiate from a closer distance from the pylon top and radiates outwards to the deck

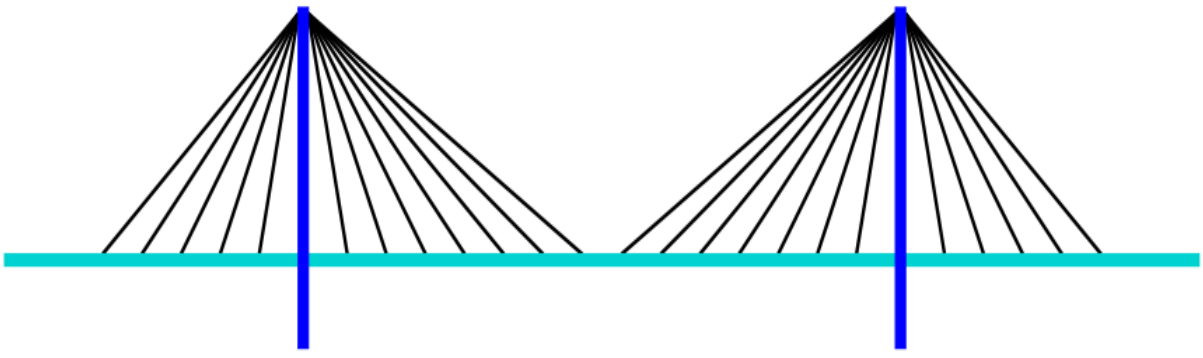

Fig 1.1: Fan type cable stayed bridges (Neils and Christos, 2012)

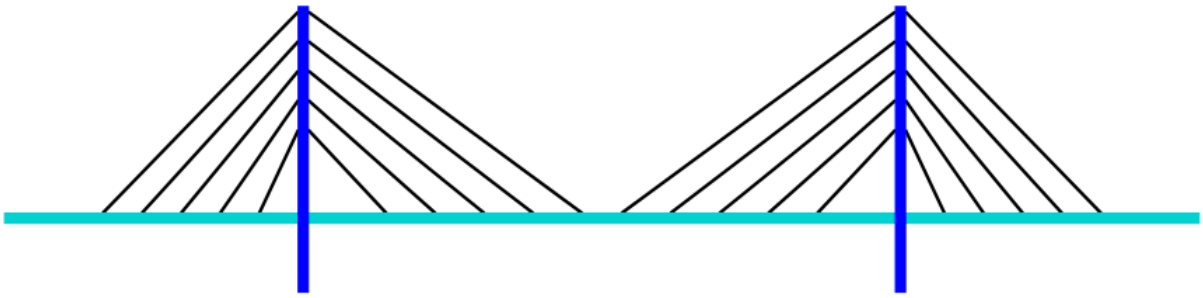

Fig 1.2: Harp type cable stayed bridges. (Neils and Christos, 2012)

The structural system of cable stayed bridges can be divided into four main components

i. The deck
ii. The cable system
iii. The pylons
iv. The anchor blocks supporting the cable system vertically and horizontally.

The stay cable anchorages at the deck will generally be spaced equidistantly so in cases where side spans are shorter than half of the main span the number of stay cables leading to the main span will be greater than the number of stay cables leading to the side span. In that case the anchor cable from the pylon tops to the anchor piers will often consists of several closely spaced individual cables.

In harp system the number of cables leading to the main span will have to be the same as in the side spans. With the anchor pier positioned at the end of the side span harp, the length of the side span will be very close to half of the main span length. That might prove inconvenient in relation to the overall stiffness of the system. It can be advantageous to position the anchor pier inside the side span harp.

The most common type of cable supported bridge is the three span bridges with a large main span flanked by two smaller side spans. However, especially within cable stayed bridges, there are also examples of a symmetrical arrangement with two main spans of equal size or an asymmetrical two-span arrangement with a long main span and a somewhat shorter side span. If the two spans are of equal, it will be necessary to stabilize the pylon top with two anchor cables

whereas the asymmetrical arrangement often can be made only one anchor cable in the shorter span.

The vast majority of cable supported bridges are built with three or two spans, but in a few cases this has not been sufficient. A straight forward solution that maintains the advantage of the three span configurations is then to arrange two or more three span bridges in sequence. In appearance the bridge will have every second opening between pylons without a central pier and the other and the other openings with a central anchor pier.

In many cases, a true multi- span cable stayed bridge will be preferable to a series of three span bridges from the point of view of appearance and function. However, from a structural viewpoint, the true multi-span arrangement presents a number of problems.

Due to the lack of anchor cables leading from vertically fixed points at the deck level to the pylon tops, the pylon must possess a considerable flexural stiffness to be able to withstand a loading condition with traffic load in only one of the two spans adjacent to the pylon. In such a loading condition, the cable pull from the loaded span will be larger than from the unloaded span so the pylon must be able to withstand the difference between the horizontal force from the cable system in loaded span and in the unloaded span.

In the early cable stayed bridges built the distance between cable anchorages at deck level is generally chosen to be quite large and as a consequence each stay cable had to carry a considerable load. It is therefore necessary to compose each stay of several prefabricated strands joined together

It is necessary to let the multi-strand cable pass over the pylon on a saddle as the space available did not allow the splitting and individual anchoring of each strand and at deck the anchoring of multi-strand made it absolutely necessary to split it into individual strands.

In modern cable stayed bridges the number of stay cables is generally chosen to be so high that each stay can be made as a mono-strand. This will ease installation, and particularly replacement, and it will render a more continuous support to the deck.

With the multi-cable system it will be possible to replace the stays one by one if the deck is designed for it, which will often be required in the design specifications. The advantages gained

in the relation to erection, maintenance and replacement have to some extent been set against an increased tendency for the stays in a multi-cable system to suffer from wind-induced vibrations.

Besides the configuration of the cables, the cable supported bridges can also be distinguished by the way cable system is anchored at the end supports. In the self – anchored system, the horizontal component of the cable force in the anchor cable is transferred as compression in the deck, whereas vertical component is taken by the anchor pier. In the earth anchored systems, both the vertical and the horizontal components of the cable force are transferred to the anchor block.

In principle, both earth anchoring and self-anchoring can be used in suspension bridges as well as cable stayed bridges. However in actual practice earth anchoring is primarily used for suspension bridges and self-anchoring for cable-stayed bridges.

In the transverse direction of the bridge, a number of different solutions for the arrangement for cable systems can be found. The arrangement used traditionally in suspension bridges comprises two vertical cable planes supporting the deck along the edges of the bridge deck. In this arrangement the deck is supported by the cable systems both vertically and torsionally.

In cases where the bridge deck is divided into three separate traffic areas the two vertical cable planes might be placed between the central area and the outer and the outer areas. This arrangement is especially attractive if the ventral area is subjected to heavy loads that would induce large sagging moment in transverse girders if the cable planes moved in from the edges towards the centre of the deck, the torsional support offered by the cable system will be drastically reduced. A more moderate displacement of the cable planes from the edges of the deck is found in bridges with cantilevered lanes for pedestrians and bicycles.

The application of more than two vertical cable planes is seen in some of the large American suspension bridges from the end of nineteenth century and the beginning of the twentieth century. In bridges with a wide bridge deck more than two cable planes could be still be considered as the moments in transverse girders will be significantly reduced.

Only one vertical cable plane has been widely used in cable stayed bridges. In this arrangement, the deck is only supported vertically by the cable system, and torsional moments must be transferred by the deck consequently, the deck must be designed with a box shaped cross section.

Inclined cable planes attached to the edges of the bridge deck and converging at top are found in cable stayed bridges with A shaped pylons. In this arrangement the deck is supported both vertically and torsionally by the cable system. Two inclined cables planes converging at top can also be supported on a single vertical pylon penetrating the deck in the central reserve or in the gap two individual box girders.

While designing cable stayed bridges following loads have to be taken into consideration, Dead load, Live load, Snow load, Impact or dynamic effect due to vehicles, Impact due to floating bodies or vessels, wind load, Longitudinal forces caused by the tractive effort of the vehicles or by braking of vehicles, Longitudinal force due to friction resistance of expansion bearings, Centrifugal force due to curvature, Horizontal force due to water currents, Buoyancy, Earth pressure including live load surcharge, Temperature effects, Deformation effects, Secondary effects, Erection stresses, Forces and effects due to earthquake and wave pressure. Among these loads all live loads and gravity loads are designed as static loads. In short span bridges even earthquake loads and wind loads are applied as modified static loads but in long span cable stayed bridges the magnitude of the loads and frequency variation necessitates these loads to be designed as dynamic loads. In case of wind loads the long span provides them enough amounts of lift forces and drag forces along with vortex formation in winds at high wind velocities to cause various complicated wind induced vibration which makes the design of bridge without analyzing for its aerodynamic effects inevitable.

1.2 BRIDGE AERODYNAMICS AND AEROELASTICITY

The first noteworthy example of a cable supported bridge failure due to wind is that of the first Dryburgh Abbey Bridge in Scotland. The cable stayed footbridge with a 79m span was designed by John and William Smith and built in 1817. In January 1818 it collapsed when several of the stay connections hooks failed during a storm. The bridge is a noteworthy example, not because of its span of or construction cost, but because of its failure – together with that of Saale River bridge in Germany in 1824- led to the demise of cable stayed bridge as a structurally efficient

solution in the minds of designers for more than a century. This was reinforced by the ensuing condemnation of cable stayed bridges by one of its conceptual fathers, Claude Navier. Oddly subsequently collapses of suspension bridges did not seem to have the same effect.

During the remainder of the century, several suspension bridge collapses and failures were witnessed during storms in Europe and North America, with a number of these described by bystanders. In most cases involved the descriptions involving undulation, twisting or oscillation implying some sort of dynamic motion in the bridge. Wind structure interaction is not considered in this period wind is considered as a static load only.

With the collapse of Tacoma Narrows Bridge a new moment in cable stayed bridge design came into existence. Aerodynamics of the bridge which was never given importance due to lack of computing power at the time was taken to be a serious thing.

The aerodynamics involved with a bridge deck can be explained as follows. Assume a bridge deck immersed in a flow of air is subjected to surface stresses induced by that flow. These surfaces stresses contribute to two kinds of forces they are Lift and Drag. Lift is the force that acts perpendicular to the direction of flow of air, lift occurs when layers of air separated by the structure travel with different velocities along the surface of the body causing differential pressures exerted on both sides of the body. Drag is the force that acts parallel to the direction of flow of air, drag occurs when the flow of air is obstructed by the structure this depends on factors such as shape, viscosity, wind velocity etc. Due to the difference between the elastic centre of lift force and centre of mass there exerts a twist or torsion in the structure which is termed as aerodynamic moment. The forces explained above are dynamic in nature which changes with respect to time hence they are generally termed as aerodynamic forces. Aero-elasticity is the discipline concerned with the study of phenomena wherein aerodynamic forces and structural motions interact significantly. In short span bridges drag force is the only force that is taken into for consideration of design wind loads and here the response is mostly static in nature. With increase in span the bridges get affected due to lift drag and twist or at times coupled with two or three forces and the response in dynamic in nature and this leads to an aerodynamic instability.

An aerodynamic instability can be a phenomenon occurring wholly within the flow alone, as when a trail of vortices or a rapidly diverging wake is shed from a fixed body. But if a body in a

fluid flow deflects under some force and the initial deflection gives rise to succeeding deflections of oscillatory or divergent character, aero-elastic instability is said to be produced. A purely aerodynamic instability such as vortex shedding may occasion structural deflection as well, initiating a phenomenon having aero-elastic character. All aero-elastic instabilities involve aerodynamic forces that act upon the body as a consequence of its motion such forces are termed self-excited.

Simiu and Scanlan, (1984) explained about all aero-elastic phenomenon. The various aero-elastic phenomenons' that occur on the bridges are given below:

i. Torsional Divergence
ii. Flutter
iii. Buffeting
iv. Vortex shedding
v. Rain-wind-induced vibrations
vi. Dry galloping
vii. Wake galloping

1.2.1 Torsional divergence

The phenomenon of torsional divergence is most closely associated with aircraft wings and their susceptibility to twisting off at some excessive air speed. To form conceptual picture of what occurs in such situations consider a thin airfoil, or any other analogous structure, such as a bridge deck, under the effect of wind the structure will be subjected to, and will act to resist, a drag force, a lift force and a twisting moment. As the wind velocity increases the twisting moment will also increase it also increases with increase in effective angle of attack of wind relative to the structure. The wind velocity at which the twisting moment increases so high that it causes collapse of the structure is called divergent velocity. This problem is quite analogous to column buckling problems where buckling occurs only at critical loads similarly divergence occurs only at certain wind velocities. The phenomenon depends upon structural flexibility and the manner in which the aerodynamic moments develop with twist. It does not depend upon ultimate structural strength.

In case of thin airfoils the aerodynamic twisting moment increases with increased angle of attack. In other, more complex forms the aerodynamic twisting moment doesn't follow the simple tendency. As a result, such structures may not follow the pattern described above; in fact depending upon the relation between aerodynamic moment and the angle of attack, some structures may be immune to torsional divergence. Finally it should be noted that in most cases of practical interest in civil engineering the critical divergent velocities are extremely high, well beyond the range of velocities normally considered in design.

1.2.2 Flutter

Flutter is one of the earliest aero-elastic oscillations to be identified in airfoils. The term flutter is widely used for many purposes but in wind engineering terms it is restricted to classical flutter, stall flutter, single degree of freedom flutter and Panel flutter.

Classical flutter the term is widely used in thin airfoils also finds its application in wind engineering. It finds its application in cable-stayed and cable-suspended bridges widely in wind engineering. It is an aero-elastic phenomenon in which two degrees of freedom rotation and vertical translation couple together in a flow driven unstable oscillation.

Stall flutter is a single degree of freedom flutter that occurs due to nonlinear characteristics of lift forces. This occurs when there is loss of lift condition. This occurs to structures where there is a huge surface area and it stops depending on the angle of approaching wind. This kind of flutter is generally observed in traffic sign posts.

A single degree of freedom flutter is an aerodynamic instability that occurs due to only one degree of freedom vibration that is continuously excited by lift forces of the oncoming wind. Single degree of freedom flutter may also include stall flutter, but it may simply be also associated with systems undergoing strongly separated flows. It is prominent among decks of cable-stayed and suspended span bridges which in various cases exhibit single degree torsional instability.

Panel flutter is a sustained oscillation of panels. These occur in side panels of large rockets caused because of high speed passage of wind along the panels. This flutter generally occurs in

supersonic flows hence these are not considered in wind engineering applications. Flutter of flags and sheets are still related to this case.

It is likely that in its detail, flutter in practically all cases involves nonlinear aerodynamics. It has been possible in a number of instances, however to treat the problem successfully by linear analytical approaches. The main reason for this are two: First the supporting structure is usually treatable as linearly elastic and its actions dominate the form of response, which is usually an exponentially modified sinusoidal oscillation. Second, it is the incipient or starting condition which may be treated as having only small amplitudes that separates the stable and unstable regimes. These two main features enable a flutter analysis to be based on the standard stability considerations of linear elastic systems.

It is characteristics of the flutter as a typical self-excited oscillation that a structural system by means of its deflection and their time derivatives taps off the energy from the wind flow. If the system is given an initial disturbance its motion will either decay or diverge according to whether the energy of motion extracted from the flow is less than or exceeds the energy dissipated by the system through mechanical damping. The theoretical dividing line between the decaying and divergent cases namely sustained sinusoidal oscillation is then recognized as the critical flutter condition.

1.2.3 Buffeting

Buffeting is the mechanism by which the fluctuations in the oncoming wind cause the bridge to vibrate. These vibrations are generally not catastrophic in nature but can be large enough to warrant closure of the bridge. Furthermore, the cumulative effect of these oscillations in the bridge over the lifetime of the bridge could be the fatigue of various components of the bridge, often leading to deterioration of structural integrity of the bridge, accompanied by large maintenance and retrofit costs.

1.2.4 Vortex shedding

Similar to buffeting, vortex-shedding is a self limiting wind-induced oscillation mechanism that is usually not of a catastrophic nature but that can generate concerns regarding the bridge's serviceability and fatigue. Unlike buffeting though, vortex shedding requires high degree of

fluid-structure interaction most often leading to oscillations that are harmonic in nature and with frequencies coinciding with those of dominant Eigen modes of the bridge.

The critical vortex shedding velocity doesn't indicate a velocity at which there is a definite propensity for a bridge to oscillate, but instead the wind velocity at which vortices shed at the same frequency as that of a particular Eigen mode. For a bridge to oscillate, several additional conditions must be met, the most important of which are low structural damping and laminar wind flow with turbulence intensities typically below 5 to 8%. Furthermore in case of a bridge girder, the wind must be nearly perpendicular to the girder axis, within a range of 20 degrees. Finally the critical wind velocity must occur at high enough wind velocities to have enough energy to excite the bridge. But also at low enough velocities that the narrowing of the wake does not disrupt the creation of vortices.

Most cable supported bridges do not suffer from vortex shedding oscillations. Nevertheless, there are several reported cases of cable supported bridges that have exhibited these oscillations, either during construction or once completed. The Longs Creek Bridge experienced up to 200mm amplitude of vibration for wind velocities between 4-11m/s at a frequency of 0.6 Hz. The Wye Bridge experienced much smaller vibration amplitudes of 44mm for wind velocities between 7.2 to 8 m/s The Soerbaelt Bridge experienced vortex induced oscillations before and after completion of the bridge, with maximum root mean square values for vertical motion of 310mm.

1.2.5 Rain-wind-induced vibrations

The exact mechanism involved in rain-wind-induced cable vibrations is not well understood, although there is enough experimental and observational evidence to suggest that the creation of one or two water rivulets along a significant length of the cable is responsible for an apparent modification in cable shape, leading to initiation of galloping.

One of the first cases of rain-wind-induced bridge cable vibrations was reported in 1986, after observations of the mechanism on the Meiko-Nishi Bridge. During the observation it was found that wind induced bridge cable vibrations always occurred in the presence of rain and for relatively moderate wind velocities between 5 to 15 m/s. Furthermore, the cable oscillations did not occur in the cable's first mode of vibration, but at modes that had frequencies in range of 1-3

Hz. Wind tunnel tests showed that the vibrations only occur when the cable is declining in direction of the wind, so main rivulet is generated on the top side of the cable.

1.2.6 Dry galloping

When wind is flowing perpendicular to a circular cylinder, the cylinder will experience a change in its drag coefficient with increasing wind velocity a large drop in drag, often referred as drag crisis. It has been observed that drag crisis leads to fluctuations in aerodynamic forces that can feed energy in structure resulting in galloping vibrations. Lightly damped cylindrical structures exposed to wind and suffering from drag crisis can vibrate violently.

1.2.7 Wake galloping

Under special circumstances and for a narrow range of wind angles of attack, structures in the wake of another object can vibrate due to special nature of the flow generated by the upstream object. This commonly referred to as wake galloping or wake buffeting. In bridges, two situations in which this can occur are for the cables behind the bridge pylon and when cables are paired or bundled.

1.2.8 Effects of Aero-elasticity

Most of the aero-elastic phenomenon such as buffeting, vortex shedding and galloping are non catastrophic in nature but still they are capable of inducing huge vibrations in the bridges which can stop the flow of traffic temporarily or damage the structural components of the bridges reducing the life of the bridge. While phenomenon such as flutter or torsional divergence are catastrophic in nature which causes immediate failure of the deck, they are also capable of producing oscillations which can cause the same effect as buffeting, vortex shedding or galloping. To control these vibrations occurring in various components of bridges various systems are developed and being used, and are discussed in the next section

1.3 CONTROL SYSTEMS

Wind tunnel tests and theoretical evaluations of the aerodynamic stability of decks and pylons do not always reveal a susceptibility for wind induced oscillations. Furthermore, Structural properties, such as damping and frequencies, are not always easily approximated before the

completion of the bridge construction. Even when the susceptibility for oscillations has been identified, aerodynamic shaping of the deck or pylon cannot always wholly eliminate them, in this case, traditional mechanical vibration control systems or guide vanes can be employed.

Vibration control systems are passive, semi-active or active in nature. They can be of the relative displacement or of the inertial type. For wind induced vibrations passive inertial systems are preferred, due to their reliability and low cost. The use of active control surfaces attached to the bridge deck to increase critical wind velocities has been proposed recently, due to their expense and complexity they are not used much but are unavoidable for ultra-long span brides. Active inertial systems has been employed extensively in Japan, ten of Japan's most recent cable supported bridges has active control, Including Akashi Kaikyo. Tokyo's rainbow bridge was the first to employ active pylon control in 1991 to counteract wind induced vibrations.

1.3.1 Shape of the girders, vented girders and cables

Designing the shape of the bridge components in the ways that are less susceptible to lift forces, drag forces and vortex formation is the most effective ways of controlling vibrations of cable supported bridges it has been found out that use of box girders instead of T beam bridges helps in eliminating torsional vibrations at lower wind velocities as box girders have higher torsional stiffness compared to others. Similarly trapezoidal or curved box girders are proved to be better in resisting vortex shedding, Flutter and buffeting response than rectangular box sections. Grooved cables are proved to be better resisting galloping and other cable induced vibrations better than the normal ones.

Even though they are capable of controlling vibrations of cables, increasing the flutter velocities of deck or controlling vibrations in pylons, they are always susceptible to flutter at higher velocities. Since the span of cable stayed bridges are evolving in time only adjusting the shape of the deck and cables become ineffective in controlling vibrations and use of mechanical dampers or control systems become inevitable

1.3.2 Tuned mass dampers

A tuned mass damper, also known as a harmonic absorber, is a device mounted in structures to reduce the amplitude of mechanical vibrations. Their application can prevent discomfort,

damage, or outright structural failure. They are frequently used in power transmission, automobiles, and buildings.

A tuned mass damper (TMD) is a device consisting of a mass, a spring, and a damper that is attached to a structure in order to reduce the dynamic response of the structure. The frequency of the damper is tuned to a particular structural frequency so that when that frequency is excited, the damper will resonate out of phase with the structural motion. Energy is dissipated by the damper inertia force acting on the structure. These are extensively used in tall pylons of cable supported bridges widely. It is used in pylons of Akashi Kaikyo Bridge which is the world's longest span cable suspension bridge in Japan and also in Taipei 101 in Taiwan which is one of the world's tallest structure.

In tuned mass dampers and hysteric tuned mass dampers the damping is a direct function of mass. Hence more mass is required for the damping to be produced for higher velocities hence the design of the girder becomes uneconomical.

1.3.3 Tuned rotary inertial damper

A tuned rotary inertial damper is a similar kind of damper as that of tuned mass damper instead of the pendulum kind of arrangement where the weight is hanged in tuned mass damper TRID system has a disc pivoted about the axis of rotation of the structure. These systems are much useful in cable stayed bridges where the motion of a structure is similar to that of a pendulum instead of horizontal vibrations.

Tuned rotary inertial damper is almost a modified version of tuned mass damper hence more mass is required for increased damping hence it also affects economical design. In addition they should be initially designed for a specific wind velocities only, hence in future cases where there is a probability of increased wind velocity may occur than the designed wind velocities these dampers become obsolete.

1.3.4 Pressurized Tuned Liquid Column Dampers

PTLCD is a U-shaped container of uniform cross sectional area with liquid filled into the container and two chambers at its ends filled with compressed air of static pressure. When the damper experiences a vibration due to structural motion, the volume of two chambers varies due

to liquid motion inside the PTLCD. The chance in volume of air chamber leads to a variation of air chamber pressure difference between the two chambers. The variation of pressure causes a delayed movement of liquids due to the smaller area of connectivity between two cylinders and thus this exerts a damping on the response of the structure.

Pressurized tuned liquid column dampers are attaché only to the supports hence in case of longer span the damping becomes inefficient and they control only torsional response of the structure the vertical motion of the structure still remains unchecked.

1.3.5 Shape Memory Alloys

Use of Shape Memory Alloys between cables to reduce wind and rain induced vibrations has been researched recently. Normal wires tend to attain huge plastic strain and they will not be effective as dampers on further vibration or displacement while shape memory alloys has the unique feature of retaining their original shape under electricity hence they can proceed the same loop of damping for number of times reaching plastic strain and retaining their original shapes.

Use of Shape Memory Alloys work good in case of cable vibrations they are inefficient in case of deck or pylon vibrations. They also have to be replaced periodically as the cycles of vibrations that can be controlled by these shape memory alloys are limited.

1.4 GYROSCOPES

A gyroscope is a mechanical device that works on the principle of law of conservation of angular momentum. A conventional gyroscope is a mechanism comprising a rotor journaled to spin about one axis, the journals of the rotor being mounted in an inner gimbal or ring; the inner gimbal is journaled for oscillation in an outer gimbal for a total of two gimbals.

The outer gimbal or ring, which is the gyroscope frame, is mounted so as to pivot about an axis in its own plane determined by the support. This outer gimbal possesses one degree of rotational freedom and its axis possesses none. The next inner gimbal is mounted in the gyroscope frame (outer gimbal) so as to pivot about an axis in its own plane that is always perpendicular to the pivotal axis of the gyroscope frame (outer gimbal). This inner gimbal has two degrees of rotational freedom.

The axle of the spinning wheel defines the spin axis. The rotor is journaled to spin about an axis, which is always perpendicular to the axis of the inner gimbal. So the rotor possesses three degrees of rotational freedom and its axis possesses two. The wheel responds to a force applied about the input axis by a reaction force about the output axis.

The behavior of a gyroscope can be most easily appreciated by consideration of the front wheel of a bicycle. If the wheel is leaned away from the vertical so that the top of the wheel moves to the left, the forward rim of the wheel also turns to the left. In other words, rotation on one axis of the turning wheel produces rotation of the third axis.

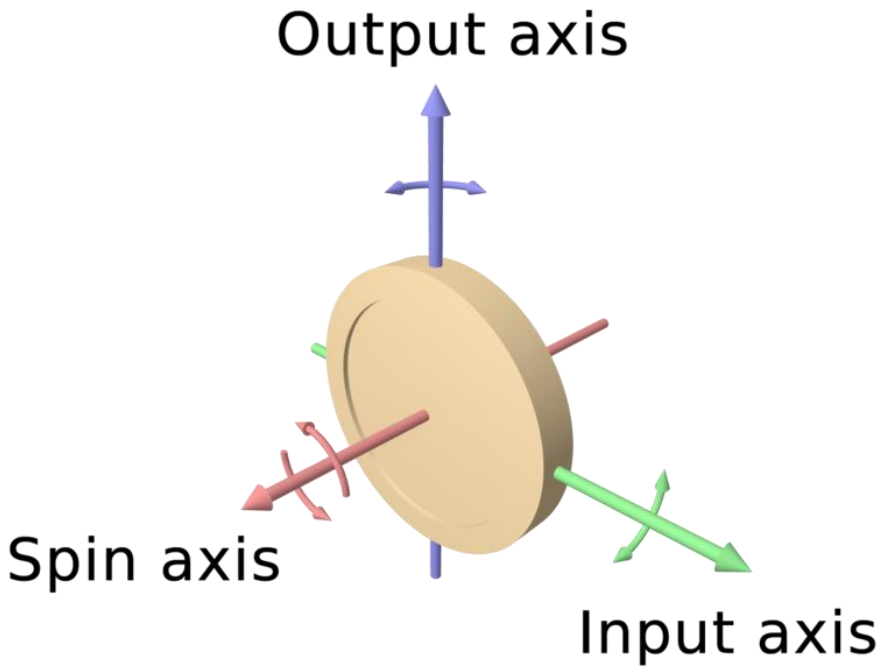

Fig 1.3: Axis denomination in gyroscopes.(Khurumi and Gupta, 2005)

A gyroscope flywheel will roll or resist about the output axis depending upon whether the output gimbals are of a free- or fixed- configuration. Examples of some free-output-gimbals devices would be the attitude reference gyroscopes used to sense or measure the pitch, roll and yaw attitude angles in a spacecraft or aircraft.

The centre of gravity of the rotor can be in a fixed position. The rotor simultaneously spins about one axis and is capable of oscillating about the two other axes, and, thus, except for its inherent resistance due to rotor spin, it is free to turn in any direction about the fixed point. Some gyroscopes have mechanical equivalents substituted for one or more of the elements. For

example, the spinning rotor may be suspended in a fluid, instead of being pivotally mounted in gimbals. A control moment gyroscope is an example of a fixed-output-gimbal device that is used on spacecraft to hold or maintain a desired attitude angle or pointing direction using the gyroscopic resistance force.

In some special cases, the outer gimbals (or its equivalent) may be omitted so that the rotor has only two degrees of freedom. In other cases, the centre of gravity of the rotor may be offset from the axis of oscillation, and, thus, the centre of gravity of the rotor and the centre of suspension of the rotor may not coincide.

1.5 GYROSCOPIC ACTIVE CONTROL DEVICES

Glassman, (1931) explained about the use of gyroscopic active control device as a ship stabilizer against roll of ships. An antiroll gyroscope works with the law of conservation of angular momentum. These ship stabilizing gyroscopes are a technology developed in the 19th century and early 20th century and used to stabilize roll motions in ocean-going ships. It lost favor in this application to hydrodynamic roll stabilizer fins because of reduced cost and weight. However, more recently (since the 1990s) a growing interest in the device has reemerged for low speed roll stabilization of vessels. The gyroscope does not rely on the forward speed of the ship to generate a roll stabilizing moment and therefore has shown to be attractive to motor yacht owners for use whilst at an anchorage.

One of the most famous ships to first use an anti-rolling gyro was the 1930 Italian passenger liner the SS Conte di Savoia which had three huge gyros to control roll.

The ship gyroscopic stabilizer typically operates by constraining the gyroscope's roll axis and allowing it to "precess" either in the pitch or the yaw axes. Allowing the gyroscope to precess as the ship rolls causes its spinning rotor to generate a counteracting roll stabilizing moment to that generated by the waves on the ship's hull. Its ability to effectively do this is dependent on a range of factors that include its size, weight and angular momentum. It is also affected by the roll period of the ship. Effective ship installations require approximately 3% to 5% of a vessel's displacement.

Unlike hydrodynamic roll stabilizing fins, the ship gyroscopic stabilizer can only produce a limited roll stabilizing moment that may be exceeded as the wave height increases. Otherwise, it is not unusual for the manufacturer to recommend that the unit not be used at sea in large waves.

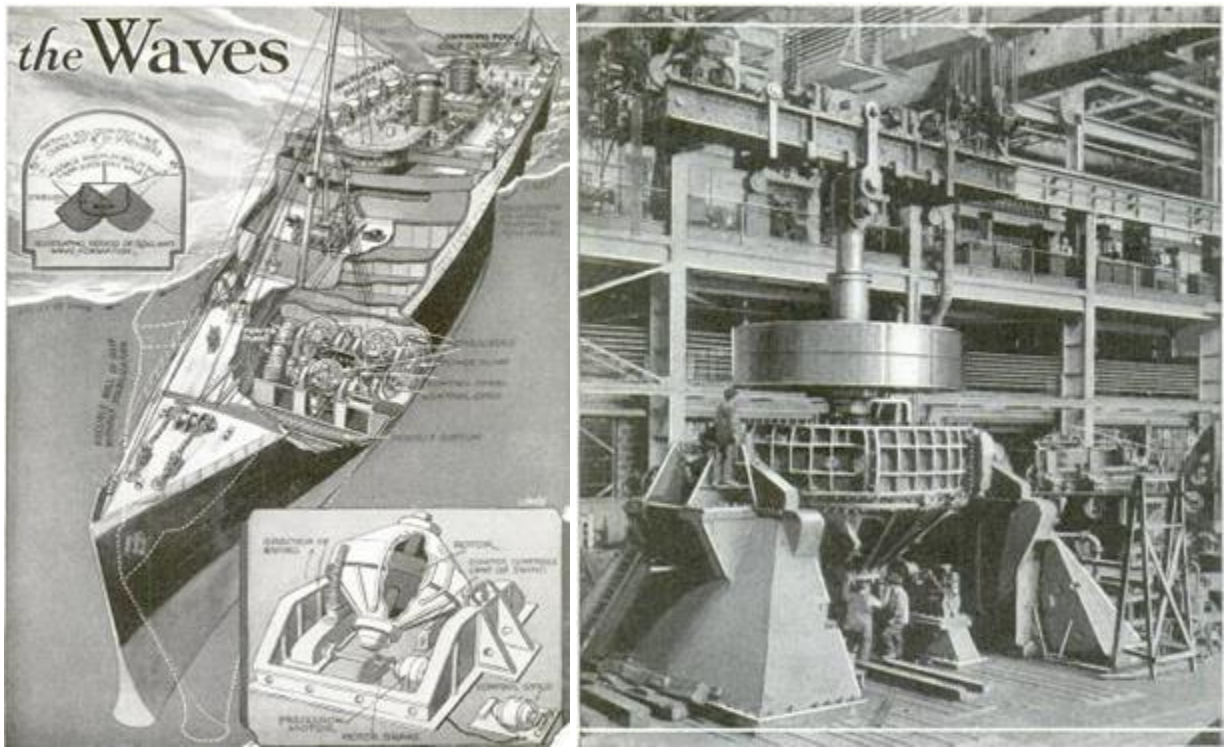

Fig 1.4: Anti roll gyroscopes installed in ships (Glassman, 1931)

1.6 USE OF GYROSCOPIC ACTIVE CONTROL DEVICES FOR DAMPING

Damping in a vibrating system provides a resistive force to that of the displacement of the structure. This force is a function of velocity at any point of time in the system that is in an active vibration. In case of torsionally vibrating system damping force in the form of a moment or couple active in the direction opposite to that of the torsional displacement and with a magnitude proportional to that of the angular velocity at that point of time.

Similarly in a gyroscopic active control system the gyroscopic reactive couple is a function of angular velocity of precision and the direction of reactive couple depends on direction of angular velocity of precision. The reactive gyroscopic couple is a function of mass moment of inertia angular velocity of the disc in gyroscope and the angular velocity of precision.

Since the direction of reactive gyroscopic couple is variable and depends on us it can be always set in direction same as that of the damping. Similarly the angular velocity of precision is controlled by us at any point of time it can be set as the same or with an additional amplification as that of the angular velocity of the deck at that time. Hence this makes the gyroscopic reactive couple to act as a damping force with mass moment of inertia, angular velocity of rotation of disc, angular velocity of deck at any point of time and the amplification factor as the variables that affect the damping provided by the device.

Compared to other damping devices they don't need complex algorithms as in case of magneto rheological fluid dampers or active tendon cable dampers this kind of dampers require simple amplifiers to provide damping. In these kind of dampers the operating frequency of rotation or amplification of precision to that of the torsional response can be controlled hence their energy spent can be optimized and based on wind velocities in condition their properties can be controlled and can resist higher wind velocities than dampers like tuned mass dampers or tuned rotary inertial dampers where the damping properties cannot be changed and hence would have a fixed flutter velocity and hence would fail in conditions where the wind velocities goes higher than flutter velocities which causes failure of structure.

1.7 OBJECTIVES OF THE PROPOSED PROJECT

The objectives of the proposed project are to study the effectiveness of the gyroscopic active control device as a damping device and simultaneously to study the operating conditions that provide highest damping. And to find out the wind velocity at which the classical flutter and single degree of freedom flutter (torsional flutter) conditions exist in a proposed cable stayed bridge section and how flutter velocities varies with increase of damping using the gyroscopic active control devices as dampers.

1.8 SCOPE OF WORK

A variety of active control systems are used for various structures such as tall buildings, pylons, bridge deck etc. currently to control various dynamic response of structures such as wind or earthquake. This gyroscopic active control system can be used as a retrofitting measure or control system for future long-span cable supported bridges to sustain higher wind loads in case of storms where wind velocities can reach higher velocities than the capacity of the bridge. As it

is a active control system this system would consume power and incur cost of operating to operate in all cases hence it can be effectively used in cases only where there is a prediction of wind velocities exceeding the design wind speed of the structure.

1.9 ORGANIZATION OF THESIS WORK

This dissertation shows how provision of torsional damping in cable stayed brides using gyroscopic active control devices can help in increasing the resistivity of the bridge towards flutter. In chapter 2 the literature related to the topics are reviewed this deals with what are the components of a cable stayed bridges how they should be designed. It also explains about what is the various control methods are adopted for controlling deck vibrations in cable stayed bridges. Further it also explains the method used to compute the flutter velocity and what are the parameters required and how it affects flutter velocity in cable stayed bridges.

Chapter 3 discusses about the methodology adopted to design the structure what are the loads used in designing the deck. It also explains how numerical flutter solutions are calculated what are the damping ratios used how they are found out etc. Chapter 4 discusses the calculations completely for design of bridge, calculation of damping those are used in flutter velocity calculations, how they are adopted and flutter velocities for corresponding torsional damping ratios. Chapter 4 shows the conclusions based on the results and outcomes, its scope where these can be effectively adopted and future projects that can be continued based on this dissertation.

2.1 DESIGN OF CABLE STAYED BRIDGES

2.1.1 Deck

Victor, (2013) says the deck is merely supported by the cables in a suspension bridge; the deck of a cable stayed bridge is an integral part of the structure resisting the axial force and bending induced by the stay cables. For bridge width greater than 15m the spans in excess of 500m, need to reduce the dead weight prompts the use of all steel orthotropic plate deck sections. Torsion box deck section with pre-stressed concrete have been used with single plane systems can also be used or Composite deck sections can also be employed. Special attention should be devoted to the anchorage of cables to the deck. The superstructure of the main span is normally constructed using the segmental cantilever method.

The ratio of side span L_s to the main span L_m for the case of a bridge with towers on both the sides of the main span usually lays between 0.3 and 0.45, the ratio can be 0.42 for concrete highway bridges while it should not exceed 0.34 for railway bridges. This ratio influences the changes in stress in backstay cables due to variation of live load. It further influences the magnitude of vertical forces at the anchor pier, the anchor pier force decreasing with increasing L_s/L_m. The choice of L_s/L_m depends also on the local conditions of water depth and foundation.

2.1.2 Tower

Towers carry the forces imposed on the bridge to the ground. They are not replaceable during the life of the bridge. Hence they should be designed to be structurally strong, constructible durable and economical.

The towers can be

a. Single free standing tower.
b. Pair of free standing tower shafts.
c. Portal frame.
d. A-frame.
e. Diamond configuration.

When the stay cables are in one plane a single free standing tower may be adopted. In this case, the pier below the box girder should be sufficiently wide for bearings to resists the torsional moment of the superstructure. For bridges with cables in two planes the towers can be free standing pair or a portal frame with a slender bracing. An additional bracing may be introduced below the deck. The A-shaped tower and the inverted Y-shaped tower have been favored for long bridges having shallow box girder decks in regions of strong wind forces. The land take at the base can be reduced by adopting a diamond configuration.

Since the tower is the most conspicuous component in a cable stayed bridge, besides structural considerations aesthetics play a prominent part in selection of the particular shape of the tower. Sometimes additional height is provided above the point of connection for architectural considerations. Anchorages of cables at the tower should follow good order. Since the cables at the deck level are anchored along a line along the edges or at the middle of the deck, it is natural that these should end along a vertical line at edges or at the middle of the deck, it is natural that these should end along a vertical line at the tower head. In case of A-shaped anchorage line can be parallel to the tower leg. It is not desirable to spread the anchorages transversely in one layer at the tower.

The single tower or towers consisting of a pair of separate columns will be stable in the lateral direction due to the restoring force provided by the cables incase of lateral displacement due to wind forces, as long as the cable anchorages are situated at a level above the base of the tower. The tower may be designed to be hinged or fixed at the base, depending on the magnitude of the vertical loads the distribution of the cable forces. While a tower with a fixed base induces a large moment, the increased rigidity of the total structure resulting from a fixed base at the towers and the relative ease in erection as compared with a hinged base may be advantageous. On the other hand hinged base results in reduced bending in moment in the towers and may be advantageous with weak soil conditions. The towers should be slender and should have a low bending stiffness in longitudinal direction so that back stay cables will be functional in partially catering to live loads in the main towers should normally vertical.

The height of the tower should be range of 0.2 to 0.25 L_m. The higher the towers the smaller will be the quantity of steel required for the cables and the compressive forces. But it is not advantageous to increase the height beyond $0.25L_m$.

2.1.3 Cables

The stay cables constitute critical components of a cable stayed bridge, as they carry the load of the deck and transfer it to the tower and the back stay cable anchorage. So the cables should be selected with utmost care. The main requirements of stay cables are (a) high load carrying capacity (b) High and stable Young's modulus of elasticity (c) Compact cross section (d)High fatigue resistance (e) Ease in corrosion protection (f) handling convenience and (g) Low cost. The ultimate tensile strength of wire is of the order of 1600 mPa. Locked coil strands have been used in early bridges, the recent ones preference is towards the use of cables with bundles of parallel wires or parallel long lay strands. The size of the cables are selected to facilitate a reasonable spacing at the deck anchorages Parallel wire cables using 7 mm wires of high tensile steel have been adopted in second Hooghly bridge. Corrosion protection of the cables is of paramount importance. For this purpose, the steel may be housed inside a polyethylene tube which is tightly connected to the anchorages. The cables are anchored at the deck and at the tower. The anchorage at the deck is fixed and has a provision for a neoprene pad damper to damp oscillations. The length adjustment is done at the tower end.

The cables are prestressed by introducing additional tensile force in the cables in order to improve the stress in main girder and tower at the completion stage to prevent the lowering of rigidity due to sagging of cable, and to optimize the cable condition for the erection. The magnitude of prestress is determined by taking into consideration the following factors☹i) the horizontal component of each cable tension is balanced such that there is no in-plane bending of tower due to unbalance horizontal force due to dead load at completion stage; and (ii) The net force on the main girder member at the connection of the cable at the completion stage be zero.

Currently the steel used for cables have ultimate tensile strength of the order of 1600mPa. Carbon fiber cables having UTS of about 3300 mPa are under development. The latter cables are claimed to have negligible corrosion and to poses high fatigue resistance however, carbon fibre cables are currently very expensive.

2.1.4 Analysis

The cable stayed bridge with the multi-stay configuration is a statically indeterminate structure with high order of indeterminacy. The deck acts as a continuous beam on elastic supports of

varying stiffness. Bending moments in the deck and pylons increase due to second order effects due to deflection of the structure. The effects of creep shrinkage during construction and service life should be considered for concrete and composite decks. The internal force distribution in the deck and tower can be managed to be compression with minimum bending by adjustment of forces in the stay cables. A rigorous analysis considering three-dimensional space action is complex. Approximate designs can be made using a two dimensional approach. Though the cable stays show a nonlinear behavior due to large displacements, sag in cables and moment-axial force interactions in stays, girders and towers, an approximate analysis assuming linear behavior leads to satisfactory results in most cases, however, a non-linear analysis essential for very long span bridges.

2.2 FLUTTER

Simiu and Scanlan (1986) said Flutter is one of the earliest aero-elastic oscillations to be identified in airfoils. The term flutter is widely used for widely recently but in wind engineering terms it is widely restricted to classical flutter, stall flutter, single degree of freedom flutter and Panel flutter.

Classical flutter the term is widely used in thin airfoils also finds its application in wind engineering. It finds its application in cable-stayed and cable-suspended bridges widely in wind engineering. It is an aero-elastic phenomenon in which two degrees of freedom rotation and vertical translation couple together in a flow driven unstable oscillation.

Stall flutter is a single degree of freedom flutter that occurs due to nonlinear characteristics of lift. This occurs when there is loss of lift condition. This occurs to structures where there is a huge surface area and it stops depending on the angle of approaching wind. This kind of flutter is generally observed in traffic sign posts.

Single degree of freedom flutter may also include stall flutter, but it may simply be also associated with systems undergoing strongly separated flows. Prominent among these are decks of cable-stayed and suspended span bridges which in various cases exhibit single degree torsional instability.

Panel flutter is a sustained oscillation of panels. These occur in side panels of large rockets caused because of high speed passage of wind along the panels. This flutter generally occurs in supersonic flows hence these are not considered in wind engineering applications. Flutter of flags and sheets are still related to this case.

It is likely that in its detail, flutter in practically all cases involves nonlinear aerodynamics. It has been possible in a number of instances, however to treat the problem successfully by linear analytical approaches. The main reason for this are two: First the supporting structure is usually treatable as linearly elastic and its actions dominate the form of response, which is usually an exponentially modified sinusoidal oscillation. Second, it is the incipient or starting condition which may be treated as having only small amplitudes that separates the stable and unstable regimes. These two main features enable a flutter analysis to be based on the standard stability considerations of linear elastic systems.

It is characteristics of the flutter as a typical self-excited oscillation that a structural system by means of its deflection and their time derivatives taps off the energy from the wind flow. If the system is given an initial disturbance its motion will either decay or diverge according to whether the energy of motion extracted from the flow is less than or exceeds the energy dissipated by the system through mechanical damping. The theoretical dividing line between the decaying and divergent cases namely sustained sinusoidal oscillation is then recognized as the critical flutter condition. Scanlan's method of flutter analysis is explained below.

The bridge deck on smooth oncoming flow of air will be two degree of freedom displacements bending displacements and twist these are represented by h and ɵ respectively. A unit span of the deck would have mass m, mass moment of inertia I, static imbalance S which is given by the product of mass m and a distance a which separates the centre of mass to the centre of elastic centre, vertical and torsional stiffness K_h and $K_ɵ$ and damping coefficients C_h and $C_ɵ$. The equations of motion can be written as:

$$m\ddot{h} + S\ddot{ɵ} + C_h\dot{h} + K_h h = L_h \qquad [2.1]$$

$$S\ddot{h} + I\ddot{ɵ} + C_ɵ\dot{ɵ} + K_ɵ ɵ = M_ɵ \qquad [2.2]$$

Here L_h and M_θ are respectively self excited aerodynamic lift and moment about the rotation axis per unit spin. This can also be written as:

$$m[\ddot{h} + a\ddot{\theta} + 2\tau_h\omega_h\dot{h} + \omega_h^2 h] = L_h \qquad [2.3]$$

$$I[\frac{a}{r2}\ddot{h} + \ddot{\theta} + 2\tau_\theta\omega_\theta\dot{\theta} + \omega_\theta\theta] = M_\theta \qquad [2.4]$$

Here r is the radius of gyration of the body about the rotational axis, τ_h and τ_θ are damping ratios to critical and ω_h and ω_θ are natural frequencies in h and θ degrees of freedom respectively. And they are defined by:

$$\omega_h = \sqrt{\frac{Kh}{m}}$$

$$\omega_\theta = \sqrt{\frac{K\theta}{I}}$$

Various forms for the linear expressions for L_h and M_θ have been employed and classical theoretical work has used complex number forms based on the representation of flutter oscillation as having the complex form $e^{i\omega t}$. But mostly linearized are used which is given below.

$$L_h = \frac{1}{2}\rho U^2(2B)[KH_1^*(K)\frac{\dot{h}}{U} + KH_2^*(K)B\frac{\dot{\theta}}{U} + K^2H_3^*(K)\theta] \qquad [2.5]$$

$$M_\theta = \frac{1}{2}\rho U^2(2B^2)[KA_1^*(K)\ )\frac{\dot{h}}{U} + KA_2^*(K)\ B\frac{\dot{\theta}}{U} + K^2A_3^*(K)\ \theta] \quad [2.6]$$

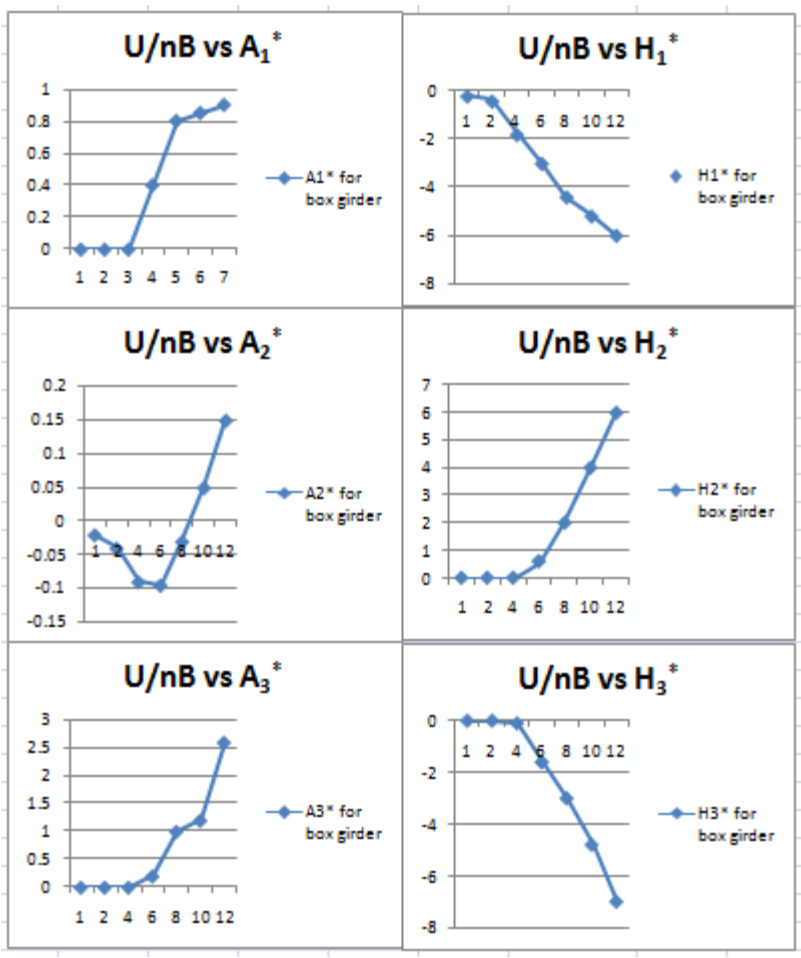

Fig 2.1: The aerodynamic coefficients H_i^* and A_i^* for a box deck section. (Simiu and Scanlan, 1986)

Where reduced frequency K is defined as:

$$\frac{U}{nB} = \frac{2\Pi}{K} \qquad [2.7]$$

B is the chord deck width or along wind dimension of the structure, U is the uniform approach velocity of the wind and ω is the circular frequency of oscillation n being the frequency of oscillation. And the coefficients H_i^* and A_i^* are non-dimensional functions of K

Because of the dependence of the aerodynamic terms upon K the analytical solution of the flutter problem becomes more involved than the comparable solution. Under K dependent conditions a typical solution method is adopted. Where a value of K is chosen and the values of H_i^* and A_i^* are obtained for respective K. It is assumed that h and ɵ have solutions proportional to $e^{i\omega t}$ which

are further inserted in equations of L_h and M_θ which are explained above. The determinant of coefficients of the amplitudes of h and θ is set equal to zero as the basic stability condition. This constitutes a complex quadratic equation in the unknown flutter frequency ω, which must then be solved. The solution obtained will in general be of the form $\omega = \omega_1 + i\omega_2$ with ω_2 not equal to zero will represent either a decaying ($\omega_2 > 0$) or a divergent ($\omega_2 < 0$) oscillation. A new value of K is chosen and the procedure is repeated until the solution is purely imaginary, that is until $\omega_2 = 0$ so that $\omega_1 = \omega$ to that solution there corresponds the flutter condition at real frequency ω_1. Let K_c be the value of K for which $\omega_1 = \omega$ the critical flutter velocity is then:

$$U_c = \frac{B\omega 1}{Kc} \qquad [2.8]$$

$$m[\ddot{h} + 2\tau_h\omega_h\dot{h} + \omega_h{}^2h] = \frac{1}{2}\rho U^2(2B)[KH_1{}^*(K)\frac{\dot{h}}{U} + KH_2{}^*(K)B\frac{\dot{\theta}}{U} + K^2H_3{}^*(K)\theta] \qquad [2.9]$$

$$I[\ddot{\theta} + 2\tau_\theta\omega_\theta\dot{\theta} + \omega_\theta\theta] = \frac{1}{2}\rho U^2(2B^2)[KA_1{}^*(K)\ )\frac{\dot{h}}{U} + KA_2{}^*(K)\ B\frac{\dot{\theta}}{U} + K^2A_3{}^*(K)\ \theta] \qquad [2.10]$$

To simplify the solution an useful variant is adopted by R.H Scanlan and J.J Tumko in which Equations [3] with [5] and [4] with [6] are compared given in equations [9] and [10], the determinant of coefficients of the amplitudes of h and θ is set equal to zero and $\frac{\omega}{\omega h} = X$ is assumed. This breaks down the equation to two quadratic equations.

From the real part:

$$X^4[1 + \frac{\rho B^4}{I}A_3{}^* - \frac{\rho B^2}{m}\frac{\rho B^4}{I}A_2{}^*H_1{}^* + \frac{\rho B^2}{m}\frac{\rho B^4}{I}A_1{}^*H_2{}^*] + X^3[2C_\theta\frac{\omega_\theta}{\omega_h}\frac{\rho B^2}{m}H_1{}^* + 2C_h\frac{\rho B^4}{I}A_2{}^*]$$
$$+ X^2[-\frac{\omega_\theta^2}{\omega_h^2} - 4C_hC_\theta\frac{\omega_\theta}{\omega_h} - 1 - \frac{\rho B^4}{I}A_3{}^*] + [\frac{\omega_\theta}{\omega_h}]^2 = 0 \qquad [2.11]$$

From the imaginary part:

$$X^3[\frac{\rho B^4}{I}A_2{}^* + \frac{\rho B^2}{m}H_1{}^* + \frac{\rho B^2}{m}\frac{\rho B^4}{I}H_1{}^*A_3{}^* - \frac{\rho B^2}{m}\frac{\rho B^4}{I}A_1{}^*H_3{}^*] + X^2[-2C_\theta\frac{\omega_\theta}{\omega_h} - 2C_h - 2C_h\frac{\rho B^4}{I}A_3{}^*]$$
$$+ X\ [-\frac{\rho B^2}{m}H_1{}^*\frac{\omega_\theta^2}{\omega_h^2} - \frac{\rho B^4}{I}A_2{}^*] + [2C_h\frac{\omega_\theta^2}{\omega_h^2} + 2C_\theta\frac{\omega_\theta}{\omega_h}] = 0 \qquad [2.12]$$

These two real equations are solved successively for different assumed values of K and their roots X are plotted vs. K. At the point where the two plots cross the flutter condition [X_c, Kc] is identified.

The above studied phenomenon is based is under the assumption that two dimensional geometric condition hold. In the case of full span bridge the deformations of the deck are the functions of position along the span so this assumption becomes invalid. Therefore a generalization of result is required for the solution.

Since flutter in its most critical condition involves the lowest frequency modes of vibration of the bridge it generally suffices to assume single modes h(x) and ɵ(x) as participants. The combined equation of [2.3] with [2.5] and [2.4] with [2.6] holds good but with few changes. Thus the equation becomes:

$$M_1[\ddot{h} + 2\tau_h\omega_h\dot{h} + \omega_h^2 h] = \frac{1}{2}\rho U^2(2B)[KC_{11}H_1^*(K)\frac{\dot{h}}{U} + KC_{12}H_2^*(K)B\frac{\dot{\theta}}{U} + K^2C_{12}H_3^*(K)\theta] \quad [2.13]$$

$$I_1[\ddot{\theta} + 2\tau_\theta\omega_\theta\dot{\theta} + \omega_\theta\theta] = \frac{1}{2}\rho U^2(2B^2)[KC_{12}A_1^*(K)\frac{\dot{h}}{U} + KC_{22}A_2^*(K)B\frac{\dot{\theta}}{U} + K^2C_{22}A_3^*(K)\theta] \quad [2.14]$$

Where:

$$M_1 = \int_0^L m(x)h^2(x)dx \quad [2.15]$$

$$I_1 = \int_0^L I(x)\theta^2(x)dx \quad [2.16]$$

$$C_{11} = \int_0^L h^2(x)dx \quad [2.17]$$

$$C_{12} = \int_0^L h(x)\theta(x)dx \quad [2.18]$$

$$C_{22} = \int_0^L \theta^2(x)dx \quad [2.19]$$

The remaining part of the solution remains the same for finding out the flutter velocity. This adopted method is apt for classical flutter in case of single degree of freedom flutter the solution is found out by the value of A_t which is given by:

$$A_t = \frac{2C_\theta I_1}{\rho C_{22}B^4} \quad [2.20]$$

Various values of A_2^* are found out for corresponding K values the value of K at which A_2^* is almost equal to A_t the value K_c is obtained. For the value of K_c critical flutter velocity U_c is found out from the following equation.

$$U_c = \frac{B\omega}{K_c} \qquad [2.21]$$

Torsional flutter velocity occurs only in case of trussed decks where the coefficient A_2^* transforms from negative to positive values for higher K values. In case of box girder bridges where A_2^* remains negative and A_t remains positive hence there exists no solution which implicates there is no existence of torsional flutter.

2.3 CONTROL SYSTEMS

Various damping systems have been proposed by various authors earlier for control of flutter and other problems related to it such as post flutter oscillations, vortex shedding etc. Few earlier proposed mechanisms are discussed here.

Preumont and Bossens (2000) presented a strategy for active damping of cable stayed bridges, using active tendons. The first part of the paper summarizes the theoretical background: the control law is briefly presented together with the main results of an approximate linear theory, which allows predicting the closed-loop poles with a root locus technique. The second part of the paper reports on experimental results obtained with a 30m long cable-stayed bridge mock-up built on the reaction wall of the ELSA test facility at the JRC Ispra (Italy); this test structure is used to demonstrate the practical implementation of the control strategy with hydraulic actuators. Finally, some potential full-scale applications are identified, concerning temporary active systems for bridges under construction, and permanent systems for suspension bridges.

Iemura and Pradono (2003) studied seismic response control of cable-stayed bridge discussed to provide special bearings at the deck-tower connections to reduce the seismic induced force and displacement. Elastic bearings plus special dampers are employed as the control devices. The dampers are the newly proposed pseudo-negative-stiffness-controlled damper. Practical advantage is that control algorithm is simple and sensors are required only at the damper to measure relative displacement and velocity. The system has been verified experimentally in the laboratory. The control algorithm commands the variable damper to produce pseudo negative

stiffness hysteretic loop. That is, unlike linear viscous damper that produces elliptical shape hysteretic loop, the controlled variable damper produces hysteretic loop that represent combination of negative stiffness and viscous damping. The point is that the combination of pseudo negative stiffness hysteretic loop plus elastic bearing stiffness produces artificial hysteretic loop that approaches rigid-perfectly plastic force-deformation characteristics which has large damping ratio. In order to study the effectiveness of this damper for seismic response control of cable-stayed bridges, application of pseudo negative stiffness damper and linear viscous damper to a typical cable-stayed bridge in Japan and to the benchmark cable-stayed bridge in the US was carried out using numerical simulations under several earthquake excitations. The results show that the pseudo negative stiffness damper reduces seismic responses better than those by passively viscous damper.

Shum et al (2008), explored the possibility of using multiple pressurized tuned liquid (MPTLCD) to reduce the wind induced vibration of long span cable-stayed bridges. By implementing a static pressure inside two sealed air champers at two ends of a traditional tuned liquid column damper (TLCD), a pressurized tuned liquid column damper (PTLCD) is formed and its natural frequency can be adjusted by not only by the length of the liquid column but also by the pressure inside its two air chambers. This special feature of PTLCD in frequency tuning greatly facilitates its application to long span cable-stayed bridges for mitigating wind induced multi modes of vibration. To further enhance the robustness and effectiveness of PTLCD for vibration control, MPTLCDs are explored in this study. The finite element model of MPTLCD id developed and incorporated into the finite element model of the cable-stayed bridge for predicting the buffeting response of the coupled MPTLCD- bridge system in the time domain. The performance of MPTLCD for suppressing combined lateral and torsional vibration of a real long span cable stayed bridge is numerically assessed. The investigations show that the MPTLCD not only provides great flexibility for selecting liquid column length but also significantly reduces the lateral and torsional displacement responses of the long span bridge under wind excitation.

Bleicher et al (2010) developed an active vibration control system for a light and flexible stress ribbon footbridge. The 13m span carbon fiber reinforced plastic stress ribbon bridge was built in the laboratory of department of civil and structural engineering Berlin institute of technology. Its lightness and flexibility result in high vibration sensitivity. To reduce pedestrian- induced

vibrations, very light pneumatic muscle actuators are placed at handrail level, introducing control forces. First a reduced discretized analytical model is derived for the stress ribbon bridge. To verify the analytical prediction, experiments without feedback control are conducted. Based on this model a delayed velocity feedback control strategy is designed. To handle the nonlinearities of muscle actuator, a subsidiary force control is designed. To handle the nonlinearities of the muscle actuator, a subsidiary feedback control strategy is implemented. Then the control performance from numerical simulation is verified by experiments under free vibration. As a result, analytical analyses agree well with experimental results. It is demonstrated that handrail-introduced forces can efficiently control the first mode response.

El-Katt et al (2011) proposed a new optimized smart control system to mitigate the cable-stayed bridge flutter due to seismic and aerodynamic vibration. A Magnetorheological (MR) fluid damper, which belongs to the class of controllable fluid dampers, is proposed for use in a control strategy for mitigating its effect on the cable-stayed bridge. Genetic algorithm is adopted to determine the flutter acceleration levels, and corresponding forces of MR dampers. The optimized forces values from MR dampers are studied under the effect of five strong earthquakes recorded, known as El-Centro, Mexico City, San Fernando, Ker Country, and Northridge earthquakes. The time delay between the monitoring system and the actuator response is also studied. The simulation and optimization results shows that the proposed control strategy using MR dampers is the promising one of the applicable control methods to reduce the seismic and aerodynamic flutter, vibration of the cable-stayed bridge.

Zhang et al (2011) studied on proposal and application of tuned rotary inertial damper abbreviated as TRID control system on long span bridges for wind induced flutter vibration control. They discussed about classical equations of motions for bridge segments and current methods of calculating flutter velocities are described. Then they derived and described the equations of damping from tuned rotary inertial damper. In this paper classical wind speed of flutter vibrations of Humen bridge is calculated using Scanlan and state space methods. Furthermore TRID control system is incorporated into system model, where TRID inertia mass can be physically installed between connections of consecutive bridge deck sections. Optimal parameters of TRID control system and their interactions, which mean tuning frequency ratio, damping ratio and rotary inertia ratio, are analyzed through numerical approaches. Base on

thorough numerical analysis, the results show that the TRID control system is feasible and effective on enhancing the flutter vibration stability of long span bridge structures, e.g. the ultimate critical wind speed of the illustration can be increased by 10% at the cost of adding additional 5% rotary inertia to the bridge structure.

Dieng et al (2012), studied the use of Nickel Titanium (Ni-Ti) shape memory alloys as damping devices to reduce vibration of cables. They quantitatively assessed the efficiency of Ni-Ti dampers to reduce the vibration amplitudes of civil engineering cables. For a practical control of the SMA in damping for stayed cables, several measurements are carried out in this work on a realistic full scale cable samople in Ifsttar (Nantes- France) Laboratory facility. The experimental observations were done inducing quite high oscillations in the middle of the cable without any damper device or with a SMA damper device made buy two thin NiTi parallel wires. The intrinsic damping coefficient in the free cables is extremely low. The reduction of cable oscillation amplitudes is about 25% in 1 min. The effects of the damper are investigated in this study, outlining the drastic reduction of the oscillation amplitudes of all along the cable in less than 10s. Other tests were performed placing the source of oscillations or damper at different positions along the cable and the results are observed and compared. Finite element simulations have been carried out using Marc/Mentrat finite element code with good agreement between experiment and simulation. The finite element fools enable to study quantitatively the effectiveness of the damper at several points of cable. The end result is clearly observed that the closer to the damping device the logarithmic decrement slope of vibration is much reduced while away from the damper it is increased and the damping power remains much higher than without damper case.

Lacarbonara et al. (2013), studied the effect of hysteric tuned mass dampers for mitigation of multi-mode flutter in long-span suspension bridges. The performance of the nonlinear absorbers is systematically compared with that of classical damped absorbers. The equations of motions from linearized parametric structural model of a suspension bridge are coupled with the equations governing the dynamics of passive nonlinear control system and the time-dependent aerodynamic loads obtained through a quasi steady nonlinear formulation and the unsteady indical theory. The equations of controlled aeroelastic system are reduced employing the Faedo-Galerkin method. Numerical simulations are performed to investigate the effectiveness of the

vibration absorbers systems comparing both the onset flutter and post flutter behavior without the control devices with the corresponding responses obtained when multiple absorbers are installed. This study compared the effective mass used in tuned mass dampers with the structure with no dampers this effectively increased the flutter velocity of 51m/s to 53m/s, 54m/s and up to 56m/s on various damping conditions that can be carried by the bridge.

2.4 MODELING OF CABLE STAYED BRIDGES

Gattulli (2008) in his paper emphasizes on various methods to be adopted for modeling cable stayed bridges. In this he gives a clear description of various methods such as single cable deck interactions, multiple cable deck interactions and Finite element modeling of cable stayed bridges.

In model for single cable deck interactions The actual planar configuration of a cable-supported cantilever beam is described, with respect to the static equilibrium configuration, by the cable displacement components Uc, Vc and the beam transverse displacements Vb within the hypothesis extensively reported. Under the assumption of small sag D to length Lc ratio, the static equilibrium configuration can be approximated by the parabolic function in the cable domain. The beam static deflection is assumed to be negligible. With respect to this reference configuration, and assuming an Euler-Bernoulli, axially rigid model of the beam, the planar configuration is completely described by the cable displacement components Uc(Xc), Vc(Xc) and the beam transverse displacements $V_b(X_b)$. We denote ω_1 the first structural modal frequency, m_b and m_c the beam and cable mass per unit length, Vg the synchronous vertical displacement imposed at both the fixed supports, C_b and C_c the transverse damping coefficient per unit length, E_b, I_b the beam flexural stiffness, E_c, A_c the cable axial stiffness, and H the mean static tension in the cable. The presented analytical model allows us to explore sources of nonlinearly induced cable vibrations, since it is able to describe large cable oscillations coupled to small beam motions.

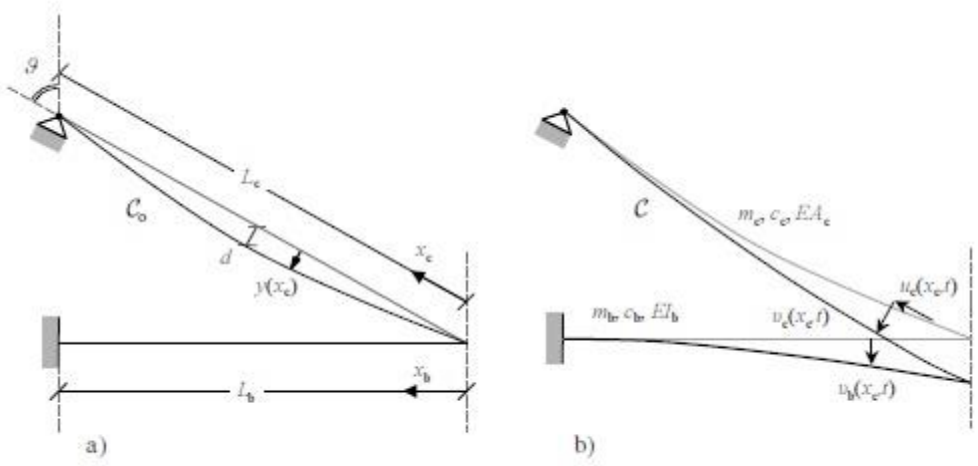

Fig 2.2: Single cable deck interaction model. (Gattuli, 2005)

In the model for multiple cable deck interactions the cable-deck interactions in a cable-stayed bridge may involve both the vertical and torsional deck motion and the transverse motion of many resonant cables. A discrete model made up of a principal system (SP) and two point secondary systems (SS1 and SS2) is formulated to address the problem. It might be considered the reduced-order model following from the discretization of a continuous model, in which two functions are used to describe the vertical and torsional motion of the deck, represented by the principal system, and other two functions are used instead to describe the transverse and longitudinal motion of each cable, represented by the secondary system.

The instantaneous configuration of the principal system is defined by its barycentrical vertical displacement V and rotation. The stiffness Kpi of the two springs (i=1, 2) connecting the principal system to the ground simulate the flexural and torsional stiffness of the bridge deck. The height-to-width ratio of the rectangular shape and the mass density can be independently tuned to properly capture the section inertial properties. The instantaneous configuration of each secondary system SSi (i=1, 2) is described by its vertical Vi and horizontal displacement Ui, since the rotational inertia is assumed to be negligible. Two springs connect the secondary system to the principal system and the upper ground, simulating the anchorages to the deck and the (quite rigid) tower, respectively. The spring stiffnesses Ksij can be tuned to simulate the cable axial stiffness, whereas the geometric stiffness acting on the transverse motion can be considered by introducing a spring prestress Hsij (i, j=1, 2). Moving from an exact formulation

of the model finite kinematics, the Hamilton principle for prestressed structures can be applied to obtain the equations governing the free undamped oscillations of the system.

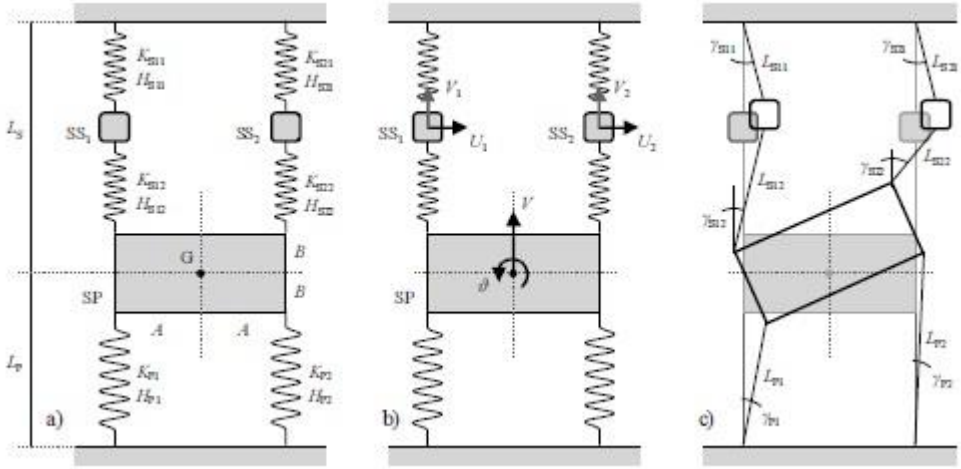

Fig 2.3: Multiple cable deck interaction model. (Gattuli, 2005)

2.5 ANGULAR MOMENTUM

Khurumi and Gupta, (2005) Angular momentum is a vector quantity that represents the product of a body's rotational inertia and rotational velocity about a particular axis. In the simple case of revolution of a particle in a circle about a center of rotation, the particle remaining always in the same plane, it is sufficient to discard the vector nature of angular momentum, and treat it as a scalar. Angular momentum can be considered a rotational analog of linear momentum. Thus, where linear momentum is proportional to mass m and linear speed ν,

$$P = m\nu$$

Angular momentum is proportional to moment of inertia I and angular speed ω,

$$L = I\omega$$

Unlike mass, which depends only on amount of matter, moment of inertia is also dependent on the position of the axis of rotation and the shape of the matter. Unlike linear speed, which occurs in a straight line, angular speed occurs about a center of rotation.

2.6 LAW OF CONSERVATION OF ANGULAR MOMENTUM

Khurumi and Gupta, (2005) Conservation follows mathematically from isotropy, or continuous directional symmetry of space, that is, no direction in space is any different from any other direction. See Noether's theorem.

A rotational analog of Newton's Third Law of Motion might be written, "In a closed system, no torque can be exerted on any matter without the exertion on some other matter of an equal and opposite torque." Hence, angular momentum can be exchanged between objects in a closed system, but total angular momentum before and after an exchange remains constant (is conserved).

Similarly, a rotational analogy of Newton's Second law of Motion might be, "A change in angular momentum is proportional to the applied torque and occurs about the same axis as that torque." Since a torque applied over time is equivalent to a change in angular momentum, then if torque is zero, angular momentum is constant. As above, a system with constant angular momentum is a closed system. Therefore, requiring the system to be closed is equivalent to requiring that no external influence, in the form of a torque, acts upon it.

A rotational analog of Newton's First Law of Motion might be written, "A body continues in a state of rest or of uniform rotation unless compelled by a torque to change its state." Thus with no external influence to act upon it, the original angular momentum of the system is conserved.

The conservation of angular momentum is used in analyzing central force motion. If the net force on some body is directed always toward some point, the center, then there is no torque on the body with respect to the center, as all of the force is directed along the radius vector, and none is perpendicular to the radius. Mathematically, torque $\tau = r \times F$ because in this case r and F are parallel vectors. Therefore, the angular momentum of the body about the center is constant. This is the case with gravitational attraction in the orbits of planets and satellites, where the gravitational force is always directed toward the primary body and orbiting bodies conserve angular momentum by exchanging distance and velocity as they move about the primary. Central force motion is also used in the analysis of the Bohr model of the atom.

For a planet, angular momentum is distributed between the spin of the planet and its revolution in its orbit, and these are often exchanged by various mechanisms. The conservation of angular

momentum in the Earth–Moon system results in the transfer of angular momentum from Earth to Moon, due to tidal torque the Moon exerts on the Earth. This in turn results in the slowing down of the rotation rate of Earth, at about 65.7 Ns/day, and in gradual increase of the radius of Moon's orbit, at ~4.5 cm/year.

The conservation of angular momentum explains the angular acceleration of an ice skater as she brings her arms and legs close to the vertical axis of rotation. By bringing part of the mass of her body closer to the axis she decreases her body's moment of inertia. Because angular momentum is the product of moment of inertia and angular velocity, if the angular momentum remains constant (is conserved), then the angular velocity (rotational speed) of the skater must increase.

The same phenomenon results in extremely fast spin of compact stars (like white dwarfs, neutron stars and black holes) when they are formed out of much larger and slower rotating stars. Decrease in the size of an object n times results in increase of its angular velocity by the factor of n^2.

2.7 GYROSCOPIC COUPLE

Khurumi and Gupta, (2005) explained that a disc spinning with angular velocity with an angular velocity of ω rad/sec about an axis OX around anticlockwise direction seen from front. The plane which is parallel to the axis in which the disc is rotating is called the plane of spinning in this case it is plane YOZ. On providing a point of rotation about OY axis perpendicular to the axis of rotation the rotating disc can be rotated about another axis which is called the axis of precision. The plane in which it lies is called the plane of precision in this case it is plane XOZ.

Let: I = Mass moment of Inertia of the disc about OX axis and

ω = Angular velocity of the disc

Angular momentum of the disc = I ω

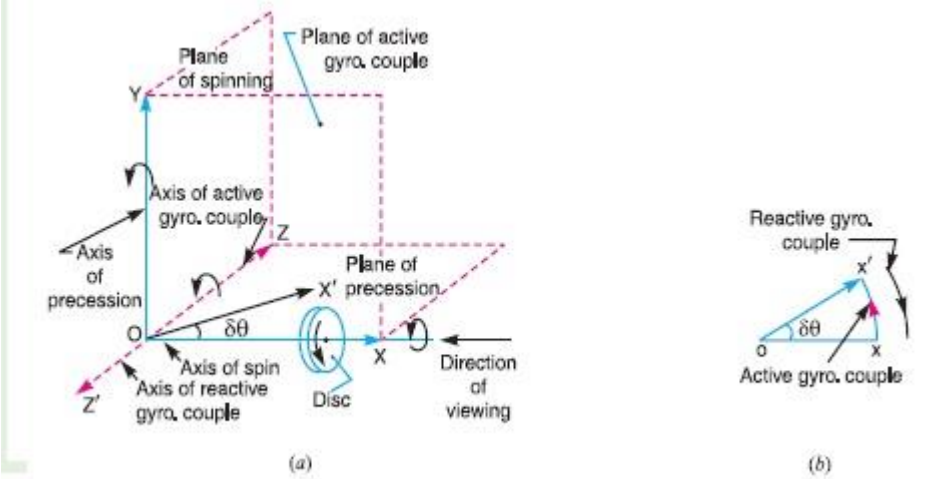

Fig 2.4: Planes and axes in gyroscope.

The angular momentum is about OX axis but the OX axis is rotating about OY axis in turn at a particular point of time OX changes to a new position OX'. The change in angle between new position and the existing position can be given by δθ. For a constant angular velocity of rotation change in angular momentum occurs.

Therefore:

$$\text{Change in angular momentum} = I\,\omega_s\,\delta\theta$$

$$\text{The rate of change of angular momentum} = I\,\omega_s\,\frac{\delta\theta}{dt}$$

The rate of change of angular momentum results in application of a couple to the disc.

The couple applied can be given by:

$$\tau = I\,\omega_s\,\omega_p$$

Where ω_p = Angular velocity of Precision

τ = Active gyroscopic couple

The active gyroscopic couple acts in a direction opposite to the precision. And the couple acts perpendicular to both axis of spinning and axis of precision. This axis about which the couple

acts is called axis of active gyroscopic couple and the plane is called the plane of active gyroscopic couple. In this case OZ acts as axis of active gyroscopic couple and the plane XOY is the plane of active gyroscopic couple.

This gyroscopic principle is used in instrument or toy known as gyroscope. Gyroscopes are installed in ships in order to minimize the rolling and pitching effect of waves. They are used in airplanes, monorail cars, gyroscopic compasses etc.

2.8 OUTCOME OF LITERATURE REVIEW

The Literature review gave an idea about various components of cable stayed bridges and how it should be designed. Neils and Christos, (2012) gave a clear view on which kind of deck is more susceptible to which kind of flutter. The paper by Gattulli (2008) clearly explained various methods on modeling the cable stayed bridges for finding natural frequency of the structure for different purposes such as single cable deck interaction for vibration in cables, multiple cable deck interaction models and finite element model for deck and pylon vibrations in addition to cable vibrations. Various other control systems are also studied such as hysteric tuned mass dampers, tuned rotary inertial dampers, multiple pressurized tuned liquid column dampers, active vibration control systems for flexible ribbon stress bridge, active tendon systems, magneto rheological fluid dampers and use of bearings in connection between cables and pylons are studied various methods used in these papers to find out the out coming advantages and disadvantages of using these systems are clearly inferred. Khurumi and Gupta, (2005) in the book "Theory of machines" gave a clear insight on how gyroscope works and how gyroscopic reactive and active couple acts in case of displacement this further helped to understand Antiroll gyro used in ship to control roll motion in ship which is similar type of displacement that occurs in torsional flutter in cable supported bridge decks. Finally Simiu and Scanlan, (1986) Gave a clear idea of how to compare the effectiveness of the torsional damping provided by the control systems would affect the flutter velocity. This gave a clear idea on how to find the flutter velocity of the structure with respect to damping provided.

3.1 GENERAL

The method which is used to solve the problem of this project is explained below.

3.2 METHODOLOGY

3.2.1 Bridge Design and modal analysis

A mid-span of cable stayed bridge with box girder deck for an overall span of 630m is designed for class A loads. The girder consists of two lanes of 4.25 m wide pavements separated by 0.5 m divider and 1.5m wide kerbs at ends. The deck is 12m wide at top flange and 7 m wide at bottom flange and has 3 box compartments with 2 vertical ribs and 2 inclined ribs and have an overall height of 2.3m. The bridge is designed for vehicle loads, dead loads such as pavement, handrails and self-weight. The deck is not designed for lateral loads as it is required that the deck should be as slender as possible for achieving least flutter velocity which would fall in the limit of the coefficients found out by Scanlan Robert and Simiu Emil for all damping values adopted and can give clear results. The study mainly emphasizes on the failure of deck on flutter, hence the design of pylons and deck are neglected as these would vary the vertical frequency of the structure more and would only make a difference in a real structure as it is a comparative study on an imaginary structure the effect would remain same on comparison.

The deck and the cables are modeled as 3d elements in staad for finding out the mode shapes and natural frequencies of the structure. Only the mid-span and cables are modeled as making it easier for modal analysis. The support of the cables are assumed rigid and taken as fixed support in model. The deck is assumed to be simply supported in both ends.

The frequencies from the structure are noted and the mode shapes and Eigen vectors are also noted at 30m intervals. The mode shapes are curve fitted in sine curves and the functions of each mode are found out. Based on the mode functions mass moment of inertia of the entire structure mass for the entire structure that has to be used in the flutter solution equations are found out.

3.2.2 Flutter velocity calculations

Quite a lot of methods are available for finding out flutter velocities in cable stayed bridges most are iterative methods and time consuming ones hence comparatively an easier method Scanlan's method is used to find out flutter velocity has been employed in finding out the critical flutter velocities. The coefficients of flutter already found out by Scanlan have been used. This method employs solving of two quadratic equations [2.13] and [2.14] whose solution gives out the ratio of flutter frequency to the vertical frequency. This frequency can be further used in equation [2.8] to find out flutter velocity. The quadratic equations further depend upon torsional damping, torsional frequency, vertical damping, vertical frequency and flutter coefficients, and quadratic equations have 4 and 3 solutions hence these merging point of both the equations in plot which gives the solution is not linear hence various torsional damping ratios are used and the solution is studied as follows.

The flutter equations are solved for real and imaginary parts of X which is the ratio of the frequency of flutter to frequency of vertical vibration. The graphs are plotted for X from real equation and X from imaginary equation vs K for various values of X. The point where X from real part and X from imaginary part coincide is noted down for the value of X_c and K_c the flutter velocity for corresponding mode is then noted. The default initial viscous damping provided by the structure is taken to be 0.2%.

3.2.3 Gyroscopic active control device

Assume the lengthwise direction of the girder as OX axis the vertical as OY axis and the horizontal direction left out perpendicular to both the axis as OZ axis. The device should contain two gyroscopes a smaller one that can be used as a sensor and a larger one that can be used as a control device that provides torsional damping.

The smaller one should be fixed to the base of the deck with pressure sensing devices like piezoelectric transducers or rosettes which can give output of electricity on application of torque. The sensor should have the axis of spinning around OY axis and axis of precision is OX. Here precision is the rotational response of the deck with respect to time. Based on the rotational response of the structure a torque or couple is applied around the axis of active gyroscopic

couple which is OZ this gives response in electric signals at the base. This measured electricity can give the angular velocity at which the bridge is rotating due to flutter or torsional divergence.

The larger one which is used as a control system has axis of spinning around OY and axis of precision around OZ. Here the electrical signals that are received from the sensor gyro are amplified to provide the same are amplified precision angle velocity to the controlling gyro. The controlling gyro's directions of precision are in same direction if the measured angular velocity of deck is in clockwise direction the angle of precision of the control gyro should also be provided in clockwise direction so that the torque is applied in the opposite direction or anticlockwise direction. Here the axis of active gyroscopic couple is OX and it acts in opposite direction to that of the torsional frequency of the box girder.

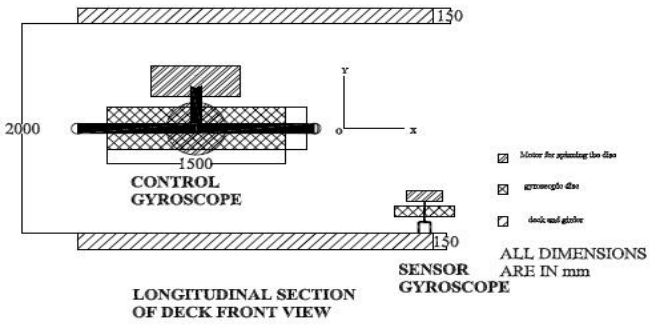

Fig 3.:1 Longitudinal section of the deck from front view

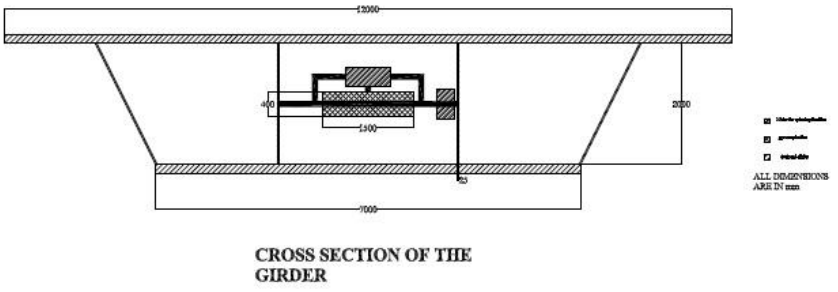

Fig 3.2: Cross section of the deck

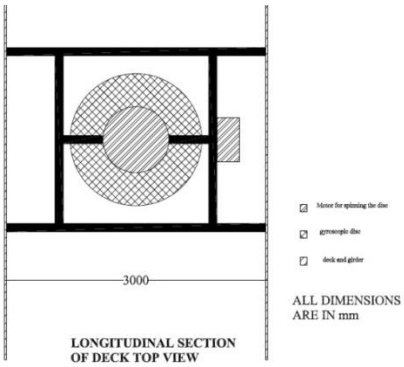

Fig 3.3: Longitudinal section of the deck from top view

Torque exerted due to torsional damping is given by:

$$\tau = C\omega_d \qquad [3.1]$$

This acts in the direction opposite to that of the angular velocity of the deck.

Here:

τ = Torque exerted on the structure due to damping.

C = Torsional damping.

ω_d = Angular frequency of the deck.

Torque exerted due to control device:

$$\tau = I\ \omega_s\ \alpha\omega_d \qquad [3.2]$$

This also acts in the direction opposite to that of the angular velocity of the deck.

Here:

τ = Torque exerted from the control device.

$\alpha = \frac{\omega p}{\omega d}$ Ratio of frequency of precision of gyroscope to torsional frequency of the deck.

For the control device at any point of time frequency of precision can be given by:

$$\omega_p = \alpha\omega_d$$

This is measured by the torque applied in the sensor gyro at any point of time and can be amplified.

Comparing [3.1] and [3.2] we can say the damping provided by the gyro at any point of time can be given by:

$$C = I \omega_s \alpha \qquad [3.3]$$

3.2.4 Properties of Gyroscopic active control device

The mass moment of inertia of disc of the gyroscope inside the deck has to be large enough to provide the maximum damping. The two factors that increase the mass moment of inertia are radius of the disc and mass of the disc mass which is also invariably a function of thickness and radius again. The thickness of the disc is inversely proportional to the radius as it is concealed in the deck of the box girder. So for various radius of the disc that can be provided inside the deck the thickness and mass moment of inertia are found out on an varying interval of 0.5m radius then the maximum moment of inertia for the respective radius is found out from this plot.

3.2.5 Calculation method

Flutter solution is found out initially for default viscous damping. Torsional damping ratio provided by using relation between critical damping, mass moment of inertia and torsional natural frequency of the structure.

$$C_{cr} = 2I_m\omega_\alpha \qquad [3.4]$$

The critical damping is found out to be 23322761.85 $kgm^2/s/rad$. This is used in estimating the damping ratios used in the structure. Since the flutter coefficients are found out only till U/nB till 12 the higher damping ratios provide no merging points of solution of X. Hence marginal increase in damping ratios in range of 0.2% is used in torsional damping. And 10 different damping ratios are used in the analysis upto 1.61358% added with the default 0.2% viscous damping added to the structure. These damping ratios are used in the flutter solutions for classical flutter solution to compare the results of flutter velocities for various torsional damping ratios. These damping ratios are also used in finding one degree of freedom flutter or torsional flutter to find out the effect of torsional damping in controlling flutter velocities.

4.1 DESIGN OF THE DECK

The deck is initially assumed to be spanning 30m between and is preliminarily assumed to be simply supported and designed for IRC class A loadings including the weight of the gyroscope. The deck is designed initially assuming simply supported as simply supported conditions would result in giving us excess bending moment than a fixed or continuous beams. This is required since the central portion of the girders of cable stayed doesn't act like a girder with continuous supports instead they give higher bending moments relatively. These initial dimensions are modeled in staad pro for checking the design of cable stayed bridge as a whole.

Steel Properties:

Yield stress of steel	=	250 N/mm^2
Allowable principal stresses in steel	=	165 N/mm^2
Allowable shear stress in steel	=	100 N/mm^2
Ultimate tensile strength of steel used in cables	=	1600 N/mm^2
Proof stress of steel used in cable	=	1280 N/mm^2

Initial assumptions:

Initially assumed volume of gyroscope (radius 1m & depth 2m)	=	6.28 m^3
Weight for the assumed volume	=	500 kN
Load due to the pavement (.075 thickness & 8.5m width)	=	14.35 kN/m
Hand rails	=	7.5 kN/m
Kerbs	=	19.69 kN/m
Assumed initial self weight (WL/300)	=	299.02 kN
Maximum shear force	=	1797.42 kN

Maximum bending moment	=	15037.995 kNm

Design of web:

Assume plate thickness	=	10mm
Required depth	=	1660.41 kN
Provide overall depth	=	2 m
Minimum web thickness based on shear considerations	=	8.99 mm

Provided thickness > required thickness

Hence Ok

Design of Flange:

Area of flange required	=	45569.69 mm^2
Width of flange	=	7 m
Thickness of flange required	=	6.51 mm
Provide flange thickness	=	25 mm
Maximum bending moment on flange plates	=	313.5 kNm
Required flange plate thickness	=	107 mm
Provide flange plate thickness	=	150 mm

Bearing stiffeners:

Maximum reaction at a support	=	7998.645 kN
Bearing area required	=	42659.44 mm
Maximum allowable width of stiffeners	=	480 mm
Provide thickness of bearing stiffener plate	=	40 mm

Width of bearing required = 272 mm

Provide 40 mm thick bearing stiffeners of 275 mm wide on both the sides of the interior webs of the box girder at supports.

Provide 40 mm thick plates covering the entire cross section of the interior of the box girder at the intersection of cables with deck.

Check for stiffeners: $\tau_{va\ cal}$

Minimum thickness of web should be greater than $\frac{d\sqrt{\tau va\ cal}}{816}$, $\frac{d\sqrt{fy}}{1344}$ or $\frac{d}{85}$

$\frac{d\sqrt{\tau va\ cal}}{816}$ = 17.33 mm

$\frac{d\sqrt{fy}}{1344}$ = 23.53 mm

$\frac{d}{85}$ = 23.53 mm

Minimum web thickness to be provided = 23.53 mm

Provided web thickness = 25 mm

Provided web thickness is greater than required hence stiffeners are not required.

Moment of Inertia about vertical axis = 4.606 m^4

Moment of Inertia about horizontal axis = 26.088 m^4

Polar moment of Inertia = 2.7812 m^4

Maximum Bending moment = 59247.5175 kNm

Maximum bending stresses in the structure = 28.07 N/mm^2

Maximum bending stress < Allowable bending stress in steel

Hence safe in flexure

Maximum Shear stress = 7998.645 kN

Maximum shear stress in structure = 2.62 N/mm^2

Maximum shear stress < allowable shear stress in steel

Hence safe

Overall main span of the deck = 630 m

Intermediate span between successive cables = 30 m

Height of the support of cables from the deck = 157.5 m

Table 4.1: Cable specifications.

Cable specification	Area of cable required (mm^2)	Diameter of the cable required (mm)	Length of the cables (m)	Un elongated length of cables (m)
1	24873.57	180	338.83	337.489
2	22944.46	180	312.58	311.439
3	21076.43	180	287.06	286.097
4	19270.42	180	262.5	261.694
5	17556.96	150	239.18	238.218
6	15966.21	150	217.5	216.704
7	14535.09	150	198	197.34
8	13316.22	150	181.4	180.846
9	12372.49	150	168.54	168.062
10	11769.99	150	160.33	159.897

The deck used for calculation has 150mm thick top flange and bottom flange and the inclined and vertical webs are 20 mm thick. The top flange is 12 m wide and bottom flange is 7m wide the top flange has 150mm over hangs on both sides from the end of attachment of inclined webs. The spacing between webs in top flange is 3 m each and bottom flange is 2 m each on spacing between outer to inner webs and 3 m between the inner webs.

Table 4.2: Natural frequencies and participation factors.

Mode	Frequency (Hz)	Period (sec)	Participation X (%)	Participation Y (%)	Participation Z (%)
1	0.441	2.266	0.000	40.675	0.000
2	0.534	1.874	0.000	0.081	0.000
3	0.645	1.551	0.000	32.150	0.000
4	0.761	1.315	0.000	0.005	0.000
5	0.847	1.181	0.000	0.000	0.000
6	0.877	1.140	0.000	16.769	0.000

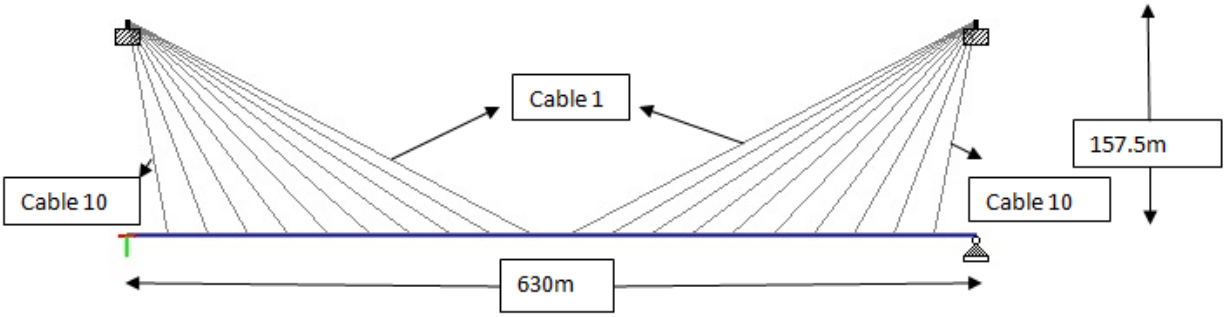

Fig 4.1: Elevation of the model.

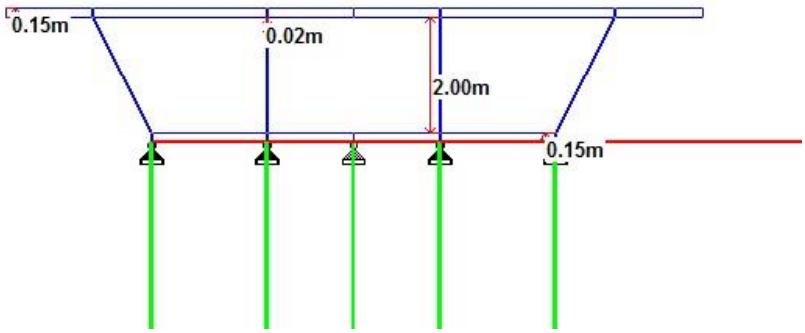

Fig 4.2: Cross section of the model

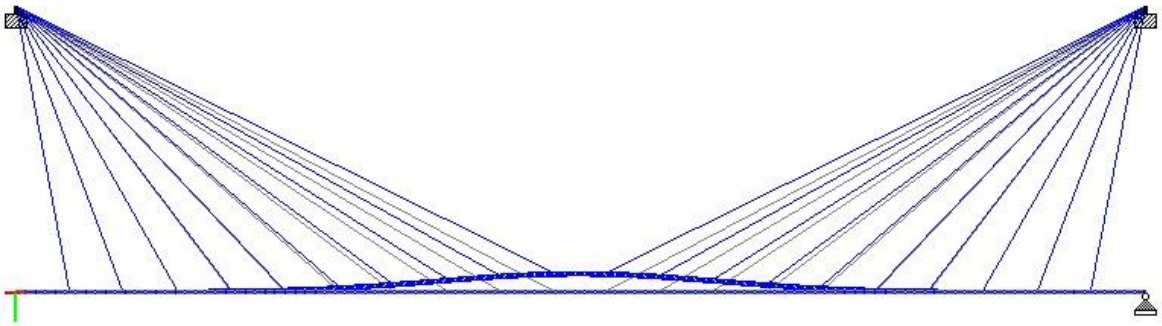

Fig 4.3: mode 1

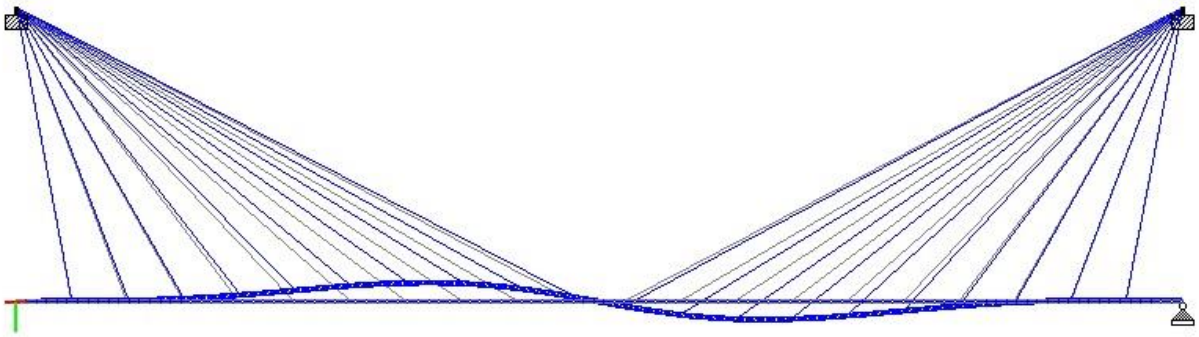

Fig 4.4: mode 2

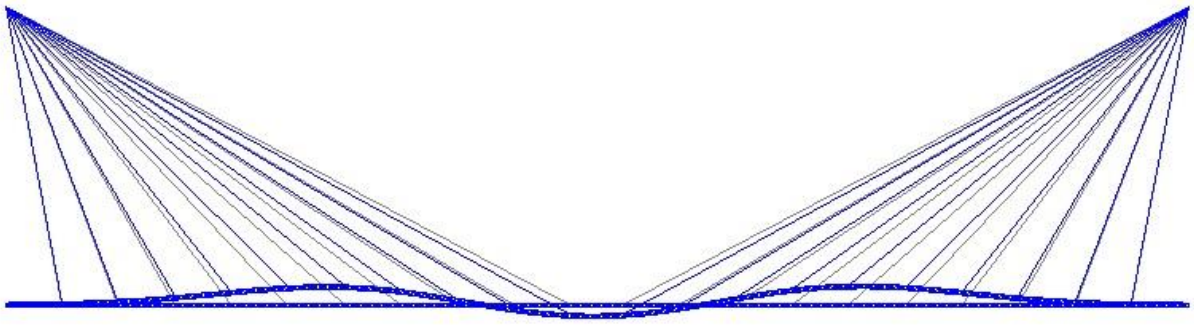

Fig 4.5: mode 3

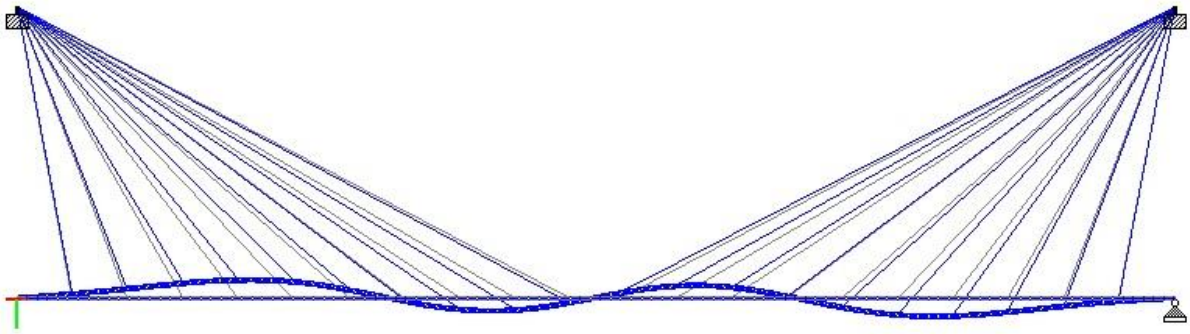

Fig 4.6: mode 4

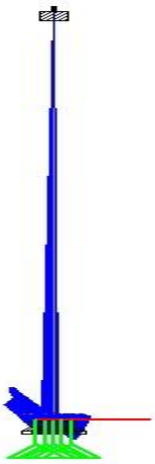

Fig 4.7: mode 5

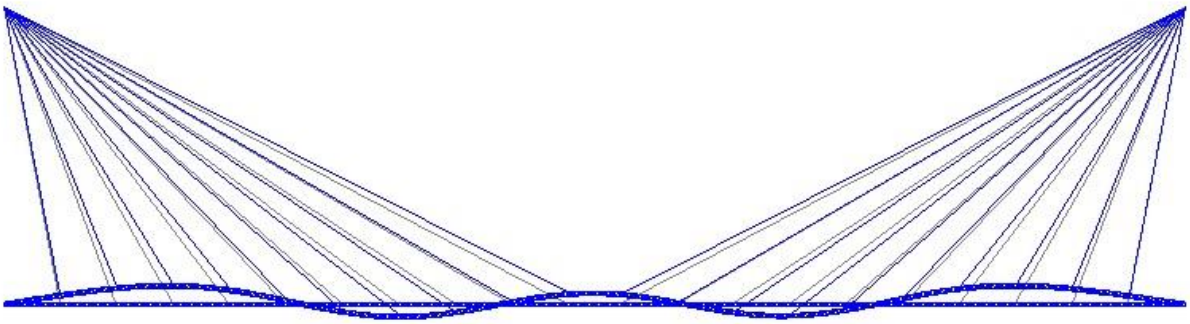

Fig 4.8: mode 6

4.2 NUMERICAL ANALYSIS

The numerical analysis is done by the method suggested by R.H Scanlan and J.J Tumko. The various properties of the bridge deck taken for the analysis are given below:

Table 4.3: Properties of the bridge deck.

Density (kg/m^3)	Mass (kg)	Mass moment of inertia (kgm^2)	Breadth (m)	Torsional damping ratio	Vertical damping ratio
1.225	24500.50964	43707.50354	12	0.2%	0.2%

The flutter derivatives for the cable stayed bridge are plotted for various values of K the modified flutter frequency for the shape of the girder.

Table 4.4: Flutter coefficients for the section.

U/nB	K	A_1^*	A_2^*	A_3^*	H_1^*	H_2^*	H_3^*
1	**6.283185**	0	-0.02	0	-0.2	0	0
2	**3.141593**	0	-0.04	0	-0.4	0	0
4	**1.570796**	0	-0.09	0	-1.8	0	-0.1
6	**1.047198**	0.4	-0.095	0.2	-3	0.6	-1.6
8	**0.785398**	0.8	-0.03	1	-4.4	2	-3
10	**0.628319**	0.85	0.05	1.2	-5.2	4	-4.8
12	**0.523599**	0.9	0.15	2.6	-6	6	-7

For a single section rested on a spring to be analyzed the above mentioned flutter derivatives are used but for a complete bridge the derivatives must taken with the factors C_{11}, C_{12} and C_{22}. These factors are which in turn functions of modal shapes are so the mode shape functions h (x) and ɵ (x) should be found out. The mode shape functions are found by fitting sine curves to the Eigen

values of the mode shapes found using the modal analysis which is already performed the Eigen values are given below for every interval of 30 m in the deck span.

Table 4.5: Eigen values at various intervals

X distance from the deck beginning	Mode 1	Mode 2	Mode 3	Mode 4	Mode 6
30	-.005	-.008	.051	.225	.462
60	-.010	-.045	.164	.500	.834
90	-.008	.143	.374	.796	.974
120	.015	.325	.652	.980	.750
150	.081	.574	.889	.886	.201
180	.205	.824	.936	.460	-.394
210	.391	.976	.704	-.139	-.664
240	.623	.953	.254	-.600	-.442
270	.845	.699	-.243	-.653	.097
300	.980	.239	-.559	-.265	.530
330	.974	-.301	-.534	.303	.510
360	.829	-.740	-.177	.661	.061
390	.603	-.961	.338	.570	-.447
420	.370	-.949	.780	.083	-.607
450	.186	-.773	.989	-.513	-.289
480	.067	-.510	.907	-.909	.308
510	.006	-.255	.645	-.962	.815
540	-.013	-.067	.354	-.744	.985
570	-.013	.039	.143	-.431	.811
600	-.006	.069	-.037	-.167	.437

Various mode shapes and their modal functions are given below:

Mode 1:

$$\lim_{187.018<x<442.982} h(x) = \sin\left(\frac{x-187.018}{1.4389}\right)$$

$$\lim_{0<x<187.018} h(x) = \frac{-\sin\left(\frac{x}{1.039}\right)}{96.577}$$

$$\lim_{442.982<x<630} h(x) = \frac{-\sin\left(\frac{x-442.982}{1.039}\right)}{96.577}$$

Mode 2:

$$\lim_{104.112<x<525.888} h(x) = \sin\left(\frac{x-104.112}{1.3677}\right)$$

$$\lim_{0<x<104.112} h(x) = \frac{-\sin\left(\frac{x}{.5784}\right)}{11.400}$$

$$\lim_{525.888<x<630} h(x) = \frac{-\sin\left(\frac{x-525.888}{.5784}\right)}{11.400}$$

Mode 3:

$$\lim_{63.0512<x<566.949} h(x) = \sin\left(\frac{x-63.0512}{1.3995}\right)$$

$$\lim_{0<x<63.0512} h(x) = \frac{-\sin\left(\frac{x}{.350}\right)}{27.024}$$

$$\lim_{566.949<x<630} h(x) = \frac{-\sin\left(\frac{x-566.949}{.350}\right)}{27.024}$$

Mode 4:

$$\lim_{0<x<630} h(x) = \sin\left(\frac{x}{0.875}\right)$$

Mode 5:

$$\lim_{0<x<630} \theta(x) = \sin\left(\frac{x}{3.5}\right)$$

Mode 6:

$$\lim_{0<x<630} h(x) = \sin\left(\frac{x}{0.7}\right)$$

Mass moment of inertia per unit length and mass per unit length of the structure are given by:

$I_m(x) = 43707.50354\ kgm^2$

$m(x) = 24500.50964\ kg$

Table 4.6: Parameters for analysis of entire length of the bridge.

Mode	M	C_{11}	C_{12}	C_{22}
1	3173298.086	129.52	157.331	315
2	5653731.802	230.759	39.026	315
3	6174036.963	251.996	-.499	315
4	7717660.549	315	-1.936×10^{-15}	315
6	7717660.549	315	0	315

Substituting the above values in solution of X in equation [2.11] and [2.12] the graphical solution of the equation is found out. For equation [2.11] all four values of X are found out of which only two are positive and for equation [2.12] all three values of X are found out in which all are positive. A graph is plotted for X real vs K and X unreal vs K based on the found out solution of X the point where both the X coincide is the critical condition for flutter. For this point corresponding X and K values are noted and which are called X_c and K_c. With corresponding value of X_c the frequency of flutter is found out ω_c. Substituting the values of ω_c and K_c in equation [2.8] we can find the flutter velocity U_c.

For undamped condition X vs K values are plotted for mode 1 2 3 4 & 5 and critical flutter condition is found out and the values are tabulated below:

Table 4.7: X vs. K for Undamped and mode 1

U/nB	X real	X unreal	K
1	1	2.84	6.283185
2	1	2.43	3.141593
4	1	2.15	1.570796
6	1	2.11	1.047198
8	1	2.11	0.785398
10	1	2.13	0.628319
12	1	2.2	0.523599

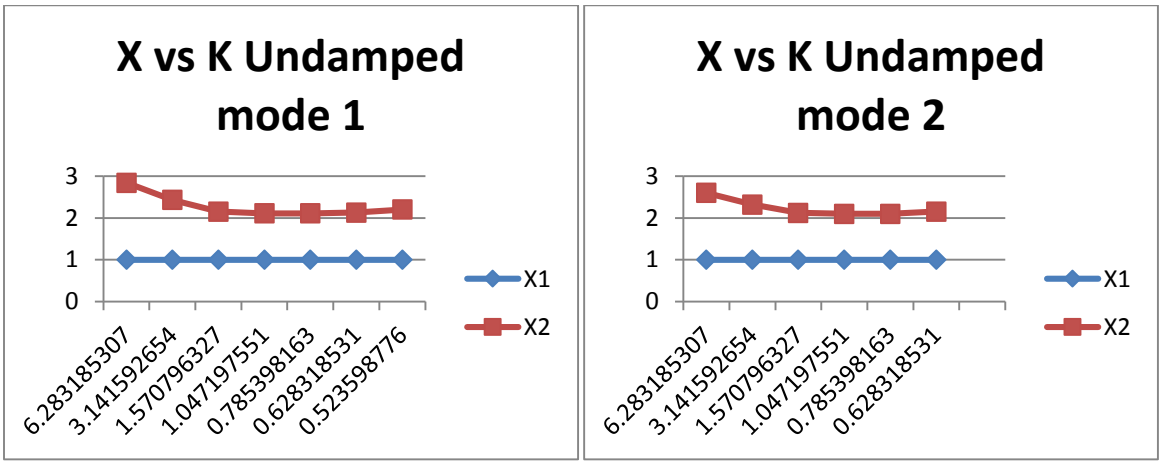

Fig. 4.9: X vs. K for Undamped and mode 1 and 2

Table 4.8: X vs. K for Undamped and mode 2

U/nB	X real	X unreal	K_c
1	1	2.6	6.283185
2	1	2.32	3.141593
4	1	2.12	1.570796
6	1	2.1	1.047198
8	1	2.1	0.785398
10	1	2.15	0.628319
12	1	2.6	0.523599

Table 4.9: X vs. K for Undamped and mode 3

U/nB	X real	X unreal	K_c
1	1	1.03	6.283185
2	1	1	3.141593
4	1	0.95	1.570796
6	1	0.94	1.047198
8	1	1	0.785398
10	0.98	1.03	0.628319
12	0.95	1	0.523599

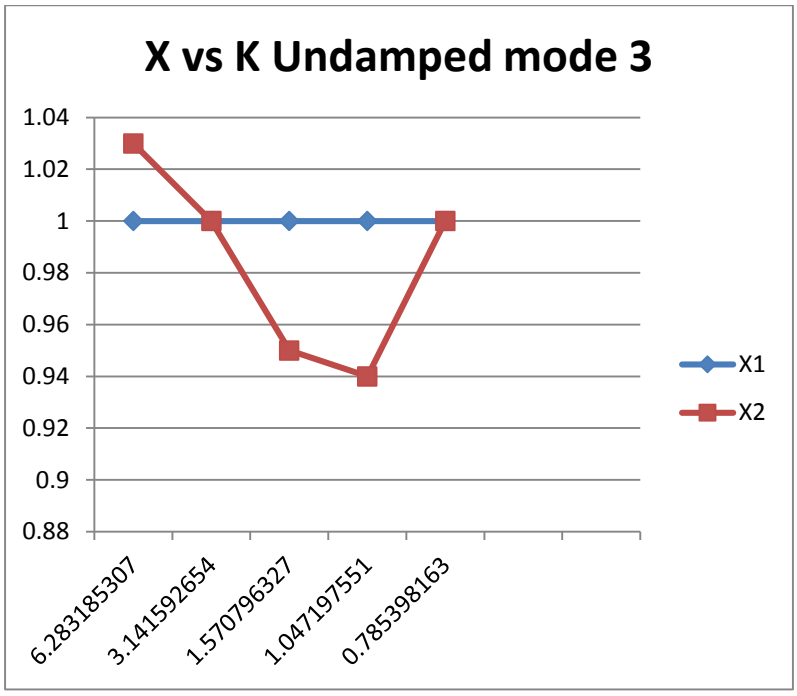

Fig. 4.10: X vs. K for Undamped and mode 3

From Fig 6 we can say that the both values of X and K coincide at the value where X is equal to 1 and K is equal to 3.141593 and hence they are X_c and K_c. This occurs with coupling of mode 3 of vertical frequency and torsional mode. By substituting the values of X_c and K_c values in eqn [2.8] we get the flutter velocity to be 55.728 km/hr.

The mass moment of inertia of disc of the gyroscope inside the deck has to be large enough to provide the maximum damping. The two factors that increase the mass moment of inertia are radius of the disc and mass of the disc mass which is also invariably a function of thickness and radius again. The thickness of the disc is inversely proportional to the radius as it is concealed in the deck of the box girder. So for various radius of the disc that can be provided inside the deck the thickness and mass moment of inertia are found out on an varying interval of 0.5m radius then the maximum moment of inertia for the respective radius is found out from this plot.

Table 4.10: Radius of disc vs. mass moment of inertia.

Radius (m)	Thickness (m)	Mass moment of inertia (kgm^2)
0.8	0.285	733.66
0.75	0.4	795.45
0.7	0.48	724.31
0.65	0.54	605.81

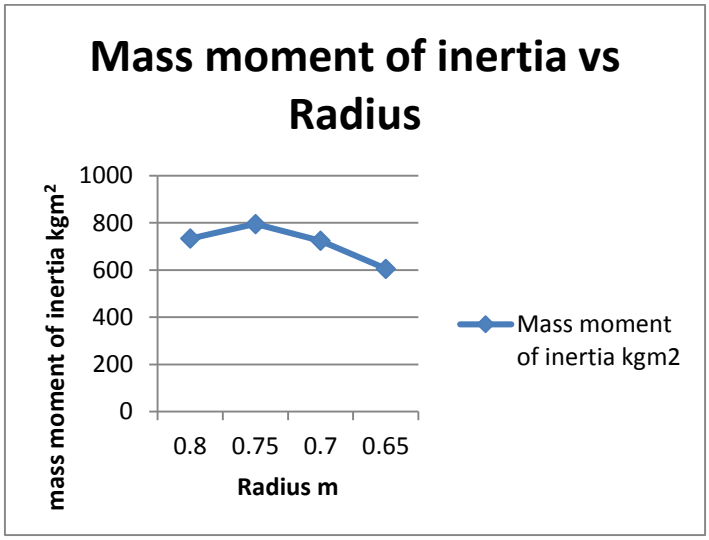

Fig 4.11: Radius of disc vs. mass moment of inertia.

From this plot it is clear that maximum mass moment of inertia when radius is 0.75m so that the thickness of the disc can be 0.4m. This gives a mass moment of inertia of 795.45 kgm^2. With this mass moment of inertia the parameters angular velocity of spinning ω_s and the ratio of angular

velocity of deck to angular velocity of precision α is changed and various damping are found out and their ratio to critical are also found out. These damping and damping ratios are tabulated below.

Table 4.11: Torsional damping properties.

S.no	Damping ratio	Damping ($kgm^2/s/rad$)	Angular frequency of spinning ω_s (rad/sec)	Ratio of precision/deck frequency α	RPM of disc	designation
1	0.00214	49977.83	62.832	1	600	A1
2	0.003214	74966.74	94.248	1	900	B1
3	0.004286	99955.66	125.664	1	1200	C1
4	0.005379	125444.1	157.708	1	1500	D1
5	0.00428	99955.66	62.832	2	600	A2
6	0.00643	149933.5	94.248	2	900	B2
7	0.008572	199911.3	125.664	2	1200	C2
8	0.010757	250888.2	157.708	2	1500	D2
9	0.00642	149933.5	62.832	3	600	A3
10	0.009642	224900.2	94.248	3	900	B3
11	0.012858	299867	125.664	3	1200	C3
12	0.016136	376332.3	157.708	3	1500	D3

Table 4.12: Final damping ratios and their designation.

Final damping ratio added with previous 0.2%	Designation
0.00414	A1
0.005214	B1
0.006286	C1 A2
0.007379	D1
0.00843	B2 A3
0.010572	C2
0.011642	B3
0.012076	D2
0.014858	C3
0.018136	D3

The above calculated damping values and damping ratios are substituted in equation [2.11] and [2.12] and the flutter velocities are found out. And the results are discussed in following chapter.

4.3 RESULTS AND DISCUSSIONS:

The found out flutter velocities for various damping ratios are plotted against the provided torsional damping and are tabulated below.

Table 4.13: Flutter velocities and their respective damping ratios.

S.no	Damping designation	Torsional damping ratio	Least flutter velocity (km/hr)	Flutter velocity (km/hr)			
				Mode 1	Mode 2	Mode 3	Mode 4
1	0.002	Undamped	55.728			55.728	223.790
2	0.00414	A1	23.814	23.814	53.423	100.310	72.983
3	0.005214	B1	40.643	40.643	63.136	133.747	89.825
4	0.006286	C1 A2	45.723	45.723	75.991	177.215	104.261

5	0.007379	D1	51.71	51.71	86.847		116.773
6	0.00843	B2 A3	57.154	57.154	97.703	229.500	135.540
7	0.010572	C2	67.412	67.412	125.830	225.917	
8	0.011642	B3	76.205	76.205		308.406	
9	0.012076	D2	76.205	76.205		222.907	
10	0.014858	C3	81.592	95.256		81.592	
11	0.018136	D3	95.817	152.410		95.817	

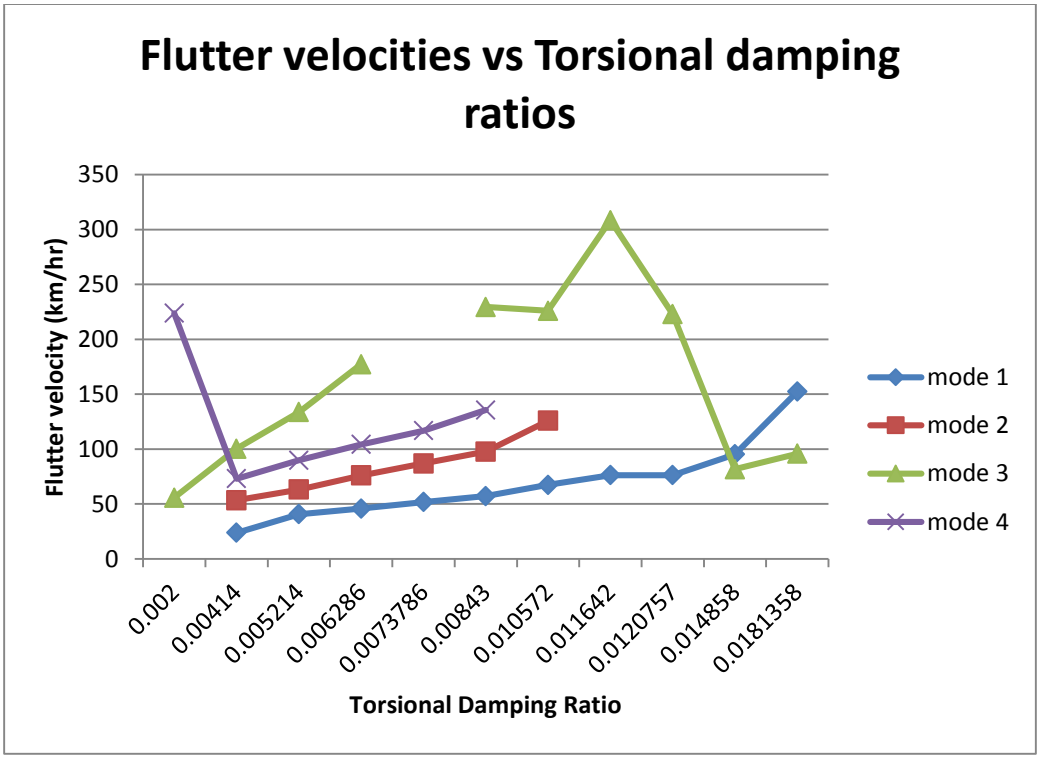

Fig 4.12: Flutter velocities in various modes.

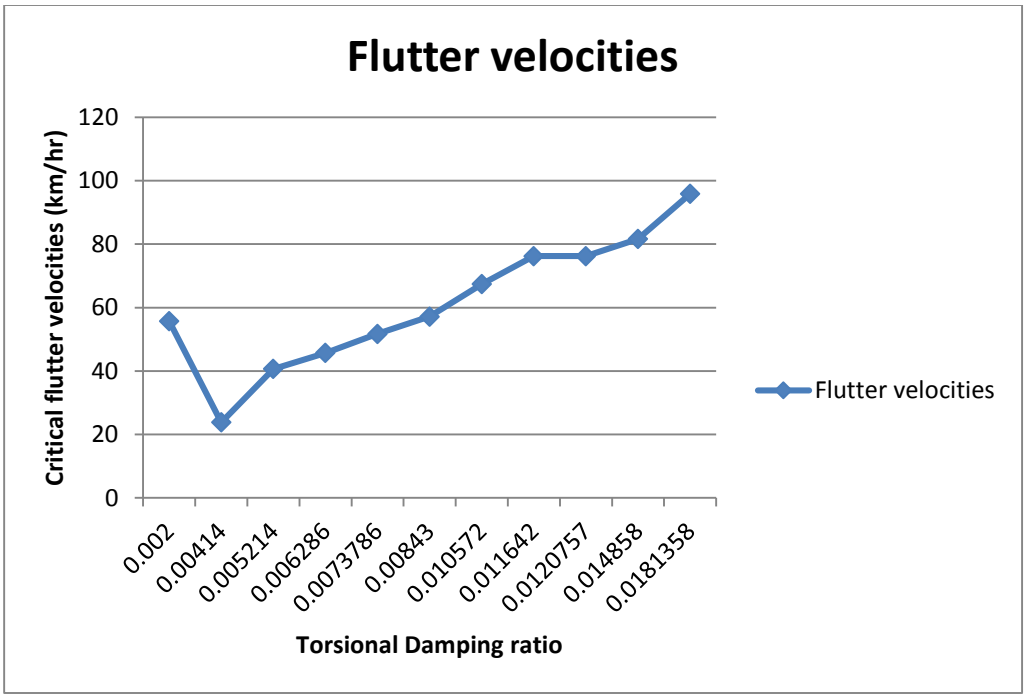

Fig 4.13: Critical flutter velocities for various damping ratios used.

The flutter velocity is found out to be 55.728 km/hr with only the initial viscous damping provided by the structure. On increasing the damping ratios to 0.414%, 0.5214%, 0.6286% and 0.73786%, the flutter velocity reduces to 23.814 km/hr, 40.643 km/hr, 45.723 km/hr and 51.71 km/hr respectively. On increasing the damping ratios to 0.843%, 1.0572%, 1.1642%, 1.20757%, 1.4858% and 1.81358% the flutter velocities are increased to 57.154 km/hr, 67.412 km/hr, 76.205 km/hr, 76.205 km/hr, 81.592 km/hr and 95.817 km/hr respectively. By increasing torsional damping ratio from 0.2% to 1.81358% the classical flutter velocity increases from 55.728 km/hr to 95.817 km/hr which is for 806.79% increase in damping ratio of initial condition flutter velocity has increased to 71.936 % still the damping ratio provided is only 1.81358% of critical.

Single degree of freedom flutter the solution is found out by the value of A_t which is given by:

$$A_t = \frac{2C_\theta I_1}{\rho C_{22} B^4}$$

Various values of A_2^* are found out for corresponding K values the value of K at which A_2^* is almost equal to A_t the value K_c is obtained. For the value of K_c critical flutter velocity U_c is found out from the following equation.

$$U_c = \frac{B\omega}{K_c}$$

Table 4.14: Torsional flutter velocities.

S.no	Damping designation	Torsional damping ratio	Torsional Flutter velocity (km/hr)
1	0.002	Undamped	322.456
2	0.00414	A1	329.131
3	0.005214	B1	332.586
4	0.006286	C1 A2	336.108
5	0.007379	D1	339.773
6	0.00843	B2 A3	343.380
7	0.010572	C2	350.968
8	0.011642	B3	354.885
9	0.012076	D2	356.497
10	0.014858	C3	367.202
11	0.018136	D3	380.668

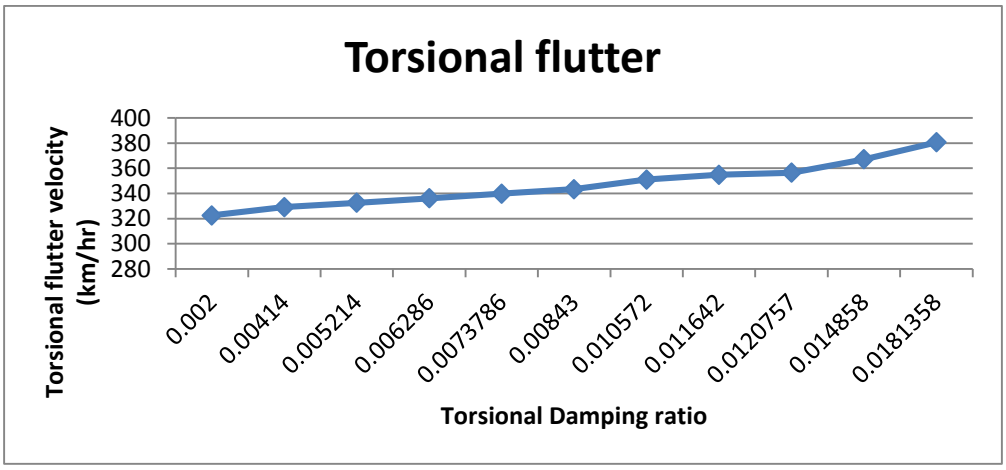

Fig 4.14: Critical torsional flutter velocities for various damping ratios.

On comparing the results for existence of one degree of freedom or torsional flutter it is found out that the torsional flutter velocity increases proportionately with increase in torsional damping. Here torsional flutter velocity is 322.456 km/hr with 0.2% damping condition and it increases to 380.668 km/hr with damping 1.81358% by increasing the damping by 806.79% the flutter velocity has been increased by 18.05%. In this case torsional or one degree of freedom flutter occurs at a far higher velocity than coupled flutter hence it is not useful as the bridge might collapse due to coupled flutter far before this condition exists. In case of other deck types as that of trussed bridges where the structure is weak against torsion torsional flutter is the predominant condition of failure hence in those conditions these gyroscopic active control systems will be more useful and effective.

This Gyroscopic active control device could be used in conditions like storm, so based on predictions of weather the operating conditions such as spinning frequency and ratio of frequency of precision to torsional frequency of the deck can be initially set so that the incoming wind velocity can be resisted by the bridge. In these kinds of equipment's the required angular frequency of spinning should be achieved with slow acceleration as higher angular acceleration can also cause higher torsion in the structure.

5. CONCLUSIONS AND RECOMMENDATIONS FOR FURTHER STUDY

5.1 GENERAL

The present study is undertaken to investigate the response of flutter velocity for classic or coupled flutter and torsional or single degree of freedom by increasing only the torsional damping achieved by gyroscopic active control device. The study is done with various damping ratios from 0.2% as the viscous damping provided by the structure for both vertical and torsional response. And the torsional damping ratios of 0.214%, 0.3214%, 0.4286%, 0.53786%, 0.643%, 0.8572%, 0.9642%, 1.0757%, 1.2858% and 1.61358% are increased with default .2%. Here the damping is increased by almost nine times to the initial default 0.2% damping which is provided by viscous damping already existing in the structure. This damping is found to be only 1.61358% of critical damping provided by only one gyroscopic active control device provided throughout the entire structure at mid-span. From the analytical results and the following conclusion can be drawn:

5.2 FLUTTER CHARECTERSTICS

- The flutter velocity is found out to be 55.728 km/hr with only the initial viscous damping provided by the structure.
- For damping ratios upto 0.7379% the flutter velocity decreases hence these cannot be used in controlling the flutter velocities
- Damping ratios from 0.843% to 1.8136% flutter velocities increases from 57.147 km/hr to 95.817 km/hr.
- For wind velocities up to 55.728 km/hr the bridge's damping is self-sufficient of controlling flutter and flutter doesn't exist.
- For wind velocities above 55.728 km/hr damping conditions 0.843% 1.0572%, 1.1642%, 1.2076%, 1.4858% and 1.8136%are capable of controlling wind velocities up to 57.154, 67.412, 76.205, 76.205, 81.592 and 95.817 respectively for the current bridge.
- For bridges which has is critical flutter conditions in single degree of freedom flutter or torsional flutter increasing the torsional damping directly increases the critical flutter capacity of bridge proportionately.

5.3 CONTROL OF FLUTTER IN EXISTING BRIDGES

- This gyroscopic active control system can be used in bridges where torsional stiffness is less and are susceptible to torsional or coupled flutter to effectively increase flutter velocity.
- This can also be used for control of other torsional oscillations due to vortex shedding etc this would be effective as it directly increases torsional damping.
- This can also be used in existing bridges in regions where higher wind velocities are possible than the designed ones.

5.4 SCOPE OF FUTURE WORK

- In this study only increase of torsional damping in structure caused by the equipment and their influence on flutter velocity is studied this can be extended by studying the position of the damping device and their response of the structure can be studied.
- Similarly only effect of single damper on mid-span is studied so the effect of adding multiple dampers and their damping properties and the response of the structure can be studied.
- Only the mid span of the model is taken in this study and the effect of other components such as pylons, foundations are ignored hence a real structure can be taken and its effect can be studied further intensively.
- Other dynamic and static aero-elastic forces such as torsional divergence, buffeting vortex induced oscillations with respect to the effect of damping forces can be studied.
- The real time response of a section or the entire model of the bridge under wind tunnels for same wind velocities or varying wind velocities or gust can be studied.

Argentini T, Pagani A, Rocchi D, Zasso A, "Monte Carlo analysis of total damping and flutter speed of a long span bridge: Effects of structural and aerodynamic uncertainties" Journal of Wind Engineering and Industrial Aerodynamics 128 (2014) 90 – 104.

Bleicher A, Schlaich M, Fujino Y, Schauer T, "Model –Based design and experimental validation of active vibration control for a stre4ss ribbon bridge using pneumatic muscle actuators" Emgomeeromg Strictires 33 (2011) 2237-2247.

Casalotti A, Arena A, Lacarbonara W, "Mititgation of post-flutter oscillations in suspension bridges by hysteric tuned mass dampers" Engineering Structures 69 (2014) 62-71.

Chen Xinzhong, Kareem Ahsan and Matsumoto Masaru, "Multimode coupled flutter and buffeting analysis of long span bridges" Journal of Wind Engineering and Industrial Aerodynamics 89 (2001) 649-664.

Chen Gen-Da and Wang Wen-Jian "3D Finite Element Model of the Bill Emerson cable-stayed bridge and its caliberation with field measured data" 4th International conference on Earthquake Engineering Taipei, Taiwan (2006) 172-181.

Cheng S.H, Lau D T, Cheung M S, "Comparison of numerical techniques for 3D flutter analysis of cables-stayed bridges" Computers and Structures 81 (2003) 2811-2822.

Dieng L, Helbert G, Chirani S A, Lecompte T, Pilvin P, "Use of Shape Memmory Alloys damper device to mitigate vibration amplitudes of bridge cables" Engineering Structures 56(2013) 1547-1556.

Duggal S K., "Design of Steel Structures" Tata McGraw hill Education Pvt. Ltd. Third Edition (2009).

El-Katt Mohamad, Shaker Raafat and Kassem Younis, "Optimum control system for Seismic and Aerodynamic Flutter Response of Cable-stayed Bridge Using Magnetorheological Dampers" Advanced materials Research vols 163-167 (2011) pp 4269-4279.

Gattuli V, “Enhanced modeling of cable – Stayed Bridge Dynamics” Saxe-Coburg Publications (2008).

Ge Y.J, Xiang H. F, “Computational models and methods for aerodynamic flutter of long-span bridges” Journal of Wind Engineering and Industrial Aerodynamics 96 (2008) 1912-1924

Gimsing Neils J., Gorgakis Christos T., “Cable Supported Bridges - Concept and Design” A John Wiley and Sons Ltd Publication, Third Edition (2012).

Glassman Don, “Popular Mechanics” Cameron Connors (April -1931).

Hua X.G Chen Z. Q, “Full-order and multimode flutter analysis using ANSYS” Finite element in analysis and Design 44 (2008) 537-551.

“IRC: 6-2000 Standard Specification and Code of Practice for Road Bridges Section II Loads and Stresses” Indian Roads congress (2000).

“IRC: 24-2010 Standard Specification and Code of Practice for Road Bridges Section V for Steel road bridges” Indian Roads congress (2010).

“IS: 800, General construction in steel code of Practice” Bureau of Indian Standards, New Delhi (2007).

Khurumi R.S, Gupta J.K, “Theory of Machines” Eurasia Publishing house 2005

Lieven N A J, Papatheodorou M, Taylor C A, “Seismic Verification of updated finite element models of cable-stayed bridges” 12th World Conference of Earthquake Engineering (2000) 2329-2336.

Nieto F, Hernandes S, Jurado J A, Mosquera A, “Analytical approach to sensitivity analysis of flutter speed in bridges considering variable deck mass” Advances in Engineering Software 42 (2011) 117-129.

Nieto F, Owen J S, Hargreaves D M, Hernandes S, “Bridge deck flutter derivatives: Efficient numerical evaluation exploiting their interdependence” Journal of Wind engineering and Industrial aerodynamics 136(2015) 138-150

Preumont Andre, Bossens Frederic "Active tendon control of cable-stayed bridges Theory and Implementation" Active structures Laboratory Universite Libre de Brixelles.

Seo Dong-Woo, Caracoglia Luca, "Estimation of torsional-flutter probability in flexible bridges considering randomness in flutter derivatives" Engineering Structures 33(2011) 2284-2296.

Shrestha Bipin "Karnali Cable-Stayed Bridge: Development of Finite Element Model and Free Vibration Analysis" Journal of Institute of Engineering, Vol 10, No. 1 pp. 14-24.

Shum K M, Xu Y L, Guo W H, " Wind – induced vibration control of long span cable-stayed bridges using multiple pressurized tuned liquid column dampers" Journal of Wind Engineering and Industrial Aerodynamics 96 (2008) 166-192.

Simiu Emil, Scanlan Robert H., "Wind effects on Structures - An Introduction to Wind Engineering" Wiley-Inter-science publications, Second Edition (1986).

Victor Johnson D., "Essentials of Bridge Engineering" Oxford & IBH Publishing Company Pvt. Ltd. (2013).

Xu F, Zhu L, Ge X, Zhang Z, "Some new insights into the identification of bridges deck flutter derivatives" Engineering Structures 75 (2014) 418-428.

Zhang C W, Li J L, Li H, Ou J P, "Preliminary Numerical Study on TRID System for Flutter Vibration Control of Bridge Structure" Procedia Engineering 14 (2011) 2796-2806.